Effective field theory for $\Lambda - \Sigma^0$ mixing in nuclear matter

H. Müller*
TRIUMF, 4004 Wesbrook Mall, Vancouver, B.C. Canada V6T 2A3
(February 9, 2008)

Abstract

We extend the effective field theory approach which successfully describes ordinary nuclei and nuclear matter to incorporate strangeness in nuclear structure. Central object is a chiral effective Lagrangian involving the baryon octet, the Goldstone boson octet, the vector meson octet and a light scalar singlet. According to the rules of effective field theory, we include all interaction terms (up to a given order of truncation) that are consistent with the underlying symmetries of QCD. We develop a mean-field approximation and study nuclear matter as a simple model for multi-strange systems. A D-type Yukawa coupling between baryons and vector mesons leads to $\Lambda - \Sigma^0$ flavor mixing in the nuclear medium. We study flavor oscillations in the nuclear matter ground state which are closely related to the phenomenon of neutrino oscillations.

PACS number(s): 21.65.+f, 13.75.Ev, 14.20.Jn, 26.60.+c

*Present address: Department of Physics, University of Colorado, Boulder, Colorado 80309

I. INTRODUCTION

Strangeness adds another, still largely unexplored, dimension to nuclear structure. On the experimental side physics of hypernuclei is approaching a phase in which not only ground state energies but also excitation spectra and electromagnetic properties are being measured [1]. To explain properties of hypernuclei, detailed information on the elementary nucleon-hyperon and hyperon-hyperon interaction is needed which, at present, is scarce and incomplete.

On the theoretical side strangeness in nuclear structure is studied from a variety of different perspectives. Microscopic meson-exchange models have been constructed which accurately reproduce the rich nucleon-nucleon and the more scarce hyperon-nucleon data [2,3]. Binding energies and single particle spectra of single hypernuclei are described in nonrelativistic [4] and relativistic [5] mean-field models. The relativistic models usually involve the baryon octet and several strange [6–8] and nonstrange mesons. A very compelling feature of the relativistic approach has been the reproduction of the observed small spin-orbit splittings of Λ hypernuclei by introducing an appropriate hyperon-meson tensor coupling [9]. Another goal of the study of strangeness in nuclear structure is to extrapolate to multi-strange systems [10]. The existence of a very large class of bound, multi-strange objects has been suggested which might be created in central collisions of very heavy ions [11].

At present, double Λ hypernuclei are the only source of information on multi-strange systems. Only a few events have been identified [1] indicating a strong attractive $\Lambda\Lambda$ interaction. While mean field models well reproduce properties of single Λ hypernuclei, theoretical uncertainties arise in extrapolations from single to multi-strange systems. The respective information on the $\Lambda\Lambda$ interaction derived from the few double Λ hypernuclei appears to be rather ambiguous. For example, nonrelativistic potential models [12] reproduce the binding energies with $\Lambda\Lambda$ potentials of completely different types.

Neutron stars are another area where the study of strangeness has received considerable attention due to the possibility of kaon condensation [13]. Uncertainties arise from an imperfect knowledge of the equation of state when hyperons are present [14]. Particularly, the question of kaon condensation is very sensitive to specific model features [15,16] related to the hyperon-nucleon and hyperon-hyperon interaction.

To summarize, a more systematic theoretical treatment of strange systems is needed to achieve more predictive power and to guide present and future experiments.

The concepts and methods of effective field theory (EFT) successfully describe the low-energy phenomenology of quantum chromodynamics (QCD). Motivated by this success, EFT concepts have recently been applied to models of nuclear structure [17]. A chiral effective Lagrangian for ordinary nuclei has lead to new insights into models based on Quantum Hadrodynamics (QHD) [18]. One important implication is that all interaction terms that are consistent with the underlying symmetries of QCD should be included.

An EFT for strange systems is more involved due to the vast number of allowed interaction terms arising form the underlying $SU(3)$ group structure. However, it is unnatural for some interaction terms to vanish without a relevant symmetry argument [19]. From this modern point of view most relativistic mean-field models which have been employed to describe strange nuclear systems (for instance [5,6,10,20]) are incomplete because only a very restricted subset of the allowed interaction terms are considered.

It is our goal to extend the ETF formulated in Ref. [17] to describe systems with strangeness. The hadronic degrees of freedom are taken to be the baryon octet, the Goldstone boson octet and the vector meson nonet. In addition a light scalar field is included which simulates the exchange of correlated pions and kaons. In an EFT approach the structure of the particles is described with increasing detail by including more and more interactions in a derivative expansion. This implies that the EFT will generally contain an infinite number of interaction terms, and one needs an organizing principle to make sensible predictions. Applications to ordinary nuclei [21] have demonstrated that the meson mean fields provide useful expansion parameters which allows a truncation of the EFT.

A framework which includes the most general types of interactions leads to new and interesting many-body effects. Most prominently, the D-type coupling between baryons and vector mesons gives rise to $\Lambda - \Sigma^0$ flavor mixing. Although it arises naturally in the EFT description flavor mixing has never been studied in this context.

To provide a first orientation of the EFT approach we will study strange nuclear matter as a simple model for multi-strange systems. The central point in the discussion is the analysis of $\Lambda - \Sigma^0$ flavor mixing. The physical nature of this effect is similar to the recently much discussed neutrino oscillations [22]. The primary result is that nuclear matter is generally in a state of mixed flavor rather than in a state with distinct Λ and Σ^0 particles. A particle interpretation is only possible in terms of the actual mass eigenstates which are a superposition of the flavor eigenstates. As a consequence, systems which contain Λ hyperons always have a small admixture of Σ^0 hyperons. Moreover, disturbing the time independent nuclear matter ground state leads to flavor oscillations characterized by distinct frequencies. Flavor mixing is driven by the mean field of the ρ meson and does not occur in isospin saturated systems. At low density the effect is very small, but we expect that signatures of this new feature will survive in heavy and very asymmetric hypernuclei. For instance, $\Lambda - \Sigma^0$ flavor mixing could produce considerable deviations of the magnetic moments from the Schmidt values [23].

The idea of $\Lambda - \Sigma^0$ mixing is not new. In the vacuum it arises from small isospin violation induced by the mass difference between up and down quarks [24] and electromagnetic interactions [25] which account for electromagnetic mass differences between members of the same isospin multiplet. Hence, explicit $SU(3)$-symmetry breaking is responsible for the mixing. In contrast, the effect we study is a true many-body effect which also arises in the chiral limit. Moreover, the effect is considerably larger than the vacuum mixing.

A systematic treatment of strangeness based on an EFT introduces a large number of coupling constants. For the parameters in the nucleon sector we rely on the studies in Ref. [17]. Ultimately, the coupling constants in the hyperon sector have to be constrained by properties of hypernuclei. Work along these lines has been reported in Ref. [20]. The couplings of the Λ hyperon were adjusted by a least square fit to experimental single particle spectra of selected hypernuclei. However, these couplings cannot be used in our framework because the analysis was based on a model which includes a very restricted subsets of the allowed interaction terms. We therefore resort to a more phenomenological approach which is based on the hyperon potential in nuclear matter. Experience has shown that different models which give a realistic description of single hypernuclei predict very similar values for the hyperon potential in nuclear matter [26,27]. Although this simple phenomenological approach cannot constrain all the relevant parameters, particularly the nonlinear meson-

meson couplings, the nuclear matter studies provide a useful qualitative description of the pertinent many-body effects.

More recently, an approach similar to ours has been proposed based on linear [7] and nonlinear [8] realization of chiral symmetry combined with the idea of broken scale invariance. Although a framework which incorporates broken scale invariance successfully describes properties of finite nuclei [21,28] the concept appears to be less compelling [29]. Compared to chiral symmetry, breaking of scale invariance is much larger on the scales relevant in nuclear structure. Symmetry breaking terms are essential for predicting masses and coupling constants and it is unclear to which extent the symmetry pattern survive at the end. Moreover, we will argue that even for the case of approximate chiral symmetry important parts of the effective theory, namely the nonlinear meson-meson interactions, appear to be rather asymmetric. The relevant couplings receive contributions from a very large number of terms in the original Lagrangian. If these couplings can be constrained by reproducing properties of normal and hypernuclei, complicated many-body effects will be included in an approximate form and it will be very difficult and also unnecessary to disentangle how these couplings arise form the underlying symmetries.

The outline of this paper is as follows: In Sec. II, we present the effective Lagrangian which lies at the heart of the EFT. Section III contains the mean field approximation. In part III B we focus on the derivation of the thermodynamic potential in the presence of $\Lambda - \Sigma^0$ flavor mixing. In part III C we present the relations that determine the equation of state. In Sec. IV we discuss how the model parameters are specified. Section V deals with strange nuclear matter as a simple model for multi-strange systems; various systems with different isospin and strangeness content are discussed, and the impact of the flavor mixing on the flavor content is illustrated. In Sec. VI, we apply our model to describe dense matter in neutron stars. In Sec. VII we study flavor oscillations in nuclear matter. Section VIII contains a short summary.

II. THE EFFECTIVE LAGRANGIAN

Recently, it has been shown that hadronic phenomenology can be combined with the ideas of EFT in form of an effective Lagrangian that realizes chiral symmetry and vector meson dominance [17,18]. This approach has been successful in describing the properties of ordinary nuclei and nuclear matter. In the following we will generalize these ideas to describe strangeness in nuclear systems. Although some of the material with restriction to the nucleon sector can be found in Refs. [17,18], we repeat it here to develop new aspects arising from the more involved $SU(3)$ structure.

The effective degrees of freedom in our approach are the baryon octet, the Goldstone boson octet and the vector meson nonet. In addition we also include a light scalar field to simulate the exchange of correlated pions and kaons. In principle, the dynamics of the non-Goldstone bosons could be generated through pion and kaon loops. In studying the many-body problem it is of advantage if the evaluation of complicated loop integrals can be avoided. Moreover, the midrange part of the baryon-baryon interaction is efficiently described by the exchange of vector mesons and a light scalar meson. In the meson sector this picture is confirmed by the observation that the coupling constants can be understood from vector meson exchange [30]. Constraints are imposed through the underlying symmetries of

QCD including Lorentz invariance, parity conservation, and approximate chiral symmetry; and all allowed interaction terms must be included. To write down a general effective theory an organizing and truncation scheme is needed for the theory to have any predictive power. Following Ref. [17] we assign to each term in the effective Lagrangian an index

$$\nu = d + \frac{n}{2} + b \ , \tag{1}$$

where d denotes the number of derivatives, n is the number of baryon fields, and b the number of non-Goldstone boson fields. Derivatives acting on baryon fields are not included in d because they generate powers of the large baryon masses, which spoil the counting scheme. In principle, an infinite number of terms is possible and a meaningful way to truncate the effective theory is needed. It has been shown that at low and moderate nuclear densities the meson mean fields and their gradients are sufficiently small to provide useful expansion parameters [21]. If one assumes that the coefficients of any term in the Lagrangian are natural, the theory can be organized in powers of the fields and their derivatives. Truncation of the Lagrangian at a given order in ν leads to a finite number of parameters which have to be determined by nuclear observables. Furthermore, if naturalness holds, the omitted higher order terms are small.

The effective degrees of freedom are introduced as nonliner realizations of the chiral group $SU(3)_L \times SU(3)_R$. For the Goldstone bosons we introduce

$$u^2 = e^{i\Pi/F_\pi} \ , \tag{2}$$

where Π is a traceless hermitian 3×3 matrix in flavor space

$$\Pi = \begin{pmatrix} \frac{1}{\sqrt{6}}\eta + \frac{1}{\sqrt{2}}\pi^0 & \pi^+ & K^+ \\ \pi^- & \frac{1}{\sqrt{6}}\eta - \frac{1}{\sqrt{2}}\pi^0 & K^0 \\ K^- & \overline{K}^0 & -\frac{2}{\sqrt{6}}\eta \end{pmatrix} \ . \tag{3}$$

The baryons are collected in a 3×3 traceless hermitian matrix B

$$B = \begin{pmatrix} \frac{1}{\sqrt{6}}\Lambda + \frac{1}{\sqrt{2}}\Sigma^0 & \Sigma^+ & p \\ \Sigma^- & \frac{1}{\sqrt{6}}\Lambda - \frac{1}{\sqrt{2}}\Sigma^0 & n \\ \Xi^- & \Xi^0 & -\frac{2}{\sqrt{6}}\Lambda \end{pmatrix} \ . \tag{4}$$

The transformation properties of the Goldstone bosons and the baryons under the chiral group are [31]

$$\begin{aligned} u &\to g_L \, u \, h^\dagger(\Pi, g) = h(\Pi, g) \, u \, g_R^\dagger \ , \\ B &\to h(\Pi, g) \, B \, h^\dagger(\Pi, g) \ , \end{aligned} \tag{5}$$

with $(g_L, g_R) \in SU(3)_L \times SU(3)_R$ and $h(\Pi, g)$ is the so-called compensator field representing an element of the conserved subgroup $SU(3)_V$. For the vector meson octet

$$V_\mu = \begin{pmatrix} \frac{1}{\sqrt{6}}V_\mu^8 + \frac{1}{\sqrt{2}}\rho_\mu^0 & \rho_\mu^+ & K_\mu^{*+} \\ \rho_\mu^- & \frac{1}{\sqrt{6}}V_\mu^8 - \frac{1}{\sqrt{2}}\rho_\mu^0 & K_\mu^{*0} \\ K_\mu^{*-} & \overline{K}_\mu^{*0} & -\frac{2}{\sqrt{6}}V_\mu^8 \end{pmatrix} \tag{6}$$

we assume the standard transformation properties of any matter field

$$V_\mu \to h(\Pi, g)\, V_\mu\, h^\dagger(\Pi, g) \ . \tag{7}$$

We also introduce a vector meson singlet S_μ and a light isoscalar scalar meson φ. The physical ω and ϕ mesons arise from the mixing relation

$$\begin{aligned} \omega_\mu &= \cos(\theta) S_\mu + \sin(\theta) V_\mu^8 \ , \\ \phi_\mu &= \sin(\theta) S_\mu - \cos(\theta) V_\mu^8 \ . \end{aligned} \tag{8}$$

The effective Lagrangian can be decomposed in two parts:

$$\mathcal{L} = \mathcal{L}_B + \mathcal{L}_M \ , \tag{9}$$

each part will contain terms up to a maximum value $\nu = 4$. The part involving the baryons is given by

$$\begin{aligned} \mathcal{L}_B = {} & \mathrm{Tr}\Big[\overline{B}(i\not{D} - M_0)B\Big] + \alpha_F \mathrm{Tr}\Big(\overline{B} i\gamma_5 [\not{\Delta}, B]\Big) + \alpha_D \mathrm{Tr}\Big(\overline{B} i\gamma_5 \{\not{\Delta}, B\}\Big) \\ & - g_F \mathrm{Tr}\Big(\overline{B}[\not{V}, B]\Big) - g_D \mathrm{Tr}\Big(\overline{B}\{\not{V}, B\}\Big) - g_S \mathrm{Tr}\Big(\overline{B}\not{S} B\Big) \\ & + \delta\mathcal{L}_B^{SB} + \cdots \ . \end{aligned} \tag{10}$$

Most terms in this part of the Lagrangian are standard [32]. The covariant derivative D_μ is defined by

$$D_\mu B = \partial_\mu B + [\Gamma_\mu, B] \ , \tag{11}$$

with the connection

$$\Gamma_\mu = \frac{1}{2}(u^\dagger \partial_\mu u + u \partial_\mu u^\dagger) \ . \tag{12}$$

In addition to the covariant derivative the baryons couple to the Goldstone bosons via

$$\Delta_\mu = \frac{1}{2}(u^\dagger \partial_\mu u - u \partial_\mu u^\dagger) \ . \tag{13}$$

The symmetry breaking part of Eq. (10) contains the quark mass matrix

$$\mathcal{M} = \mathrm{diag}\{m_u, m_d, m_s\} \tag{14}$$

and generates the baryon masses and scalar couplings

$$\begin{aligned} \mathrm{Tr}(\overline{B} M_0 B) - \delta\mathcal{L}_B^{SB} = {} & \overline{N}(M_N - g_N^s \varphi) N + \overline{\Lambda}(M_\Lambda - g_\Lambda^s \varphi)\Lambda \\ & + \overline{\mathbf{\Sigma}}(M_\Sigma - g_\Sigma^s \varphi)\mathbf{\Sigma} + \overline{\Xi}(M_\Xi - g_\Xi^s \varphi)\Xi \ . \end{aligned} \tag{15}$$

The couplings to the scalar field are purely phenomenological simulating the rather complex process of correlated two pion and two kaon exchange. The couplings g_F^s are not constrained by chiral symmetry and have to be determined for each baryon flavor separately. All the

terms in Eq. (15) can be constructed by using suitable combinations of the baryon matrix and the quark mass matrix. For the scalar couplings terms quadratic in $\mathcal{M}$ are needed, *i.e.*

$$g_F^s = \mathcal{O}(m_q^2) \ . \tag{16}$$

The terms listed in Eq. (10) are all of order $\nu \leq 2$. The ellipsis stands for terms which contain one or more derivatives of the meson fields, *e.g.* tensor couplings, and for the couplings to the electromagnetic field. Although important for finite nuclei calculations [17] these terms are not needed for our discussion of nuclear matter. Also omitted are terms which contain higher-order couplings between Goldstone bosons and contact interaction of four and more baryons. Contact interactions are taken into account by the couplings to the scalar and vector mesons [17].

The mesonic part of the Lagrangian can be written as

$$\begin{aligned}\mathcal{L}_M = &-\frac{1}{2}F_\pi^2 \mathrm{Tr}\Big(\{\Delta_\mu, \Delta^\mu\}\Big) - \frac{1}{4}\mathrm{Tr}\Big(V_{\mu\nu}V^{\mu\nu} - 2m_8^2 V_\mu V^\mu\Big) - \frac{1}{4}S_{\mu\nu}S^{\mu\nu} + \frac{1}{2}m_1^2 S_\mu S^\mu \\ &+ \frac{1}{2}(\partial_\mu\varphi\partial^\mu\varphi - m_s^2\varphi^2) + \delta\mathcal{L}_{M_1}^{SB} + \mathcal{V}(\varphi, V_\mu, S_\mu) \ ,\end{aligned} \tag{17}$$

with

$$V_{\mu\nu} = D_\mu V_\nu - D_\nu V_\mu \quad \text{and} \quad S_{\mu\nu} = \partial_\mu S_\nu - \partial_\nu S_\mu \ , \tag{18}$$

for the abelian field tensors. Explicit symmetry breaking terms are collected in $\delta\mathcal{L}_{M_1}^{SB}$ which, in analogy to the baryons, generate the physical meson masses. For the vector mesons this leads to

$$\begin{aligned}&\frac{1}{2}m_8^2\mathrm{Tr}(V_\mu V^\mu) + \frac{1}{2}m_1^2 S_\mu S^\mu + \delta\mathcal{L}_{M_1}^{SB} \\ &\qquad = \frac{1}{2}m_\omega^2\omega_\mu\omega^\mu + \frac{1}{2}m_\phi^2\phi_\mu\phi^\mu + \frac{1}{2}m_\rho^2\boldsymbol{\rho}_\mu\boldsymbol{\cdot}\boldsymbol{\rho}^\mu + m_{K^*}^2(K_\mu^{*+}K^{*-,\mu} + \overline{K}_\mu^{*0}K^{*0,\mu}) \ .\end{aligned} \tag{19}$$

Nonlinear meson-meson interactions are collected in the potential

$$\begin{aligned}\mathcal{V}(\varphi, V_\mu, S_\mu) = &-\frac{1}{3!}\kappa_3\varphi^3 - \frac{1}{4!}\kappa_4\varphi^4 \\ &+ \frac{1}{2}(\eta_1^1\varphi + \frac{1}{2}\eta_2^1\varphi^2)S_\mu S^\mu + \frac{1}{2}(\eta_1^8\varphi + \frac{1}{2}\eta_2^8\varphi^2)\mathrm{Tr}(V_\mu V^\mu) \\ &+ \frac{1}{4!}\zeta_1(S_\mu S^\mu)^2 + \frac{2}{4!}\zeta_8(\mathrm{Tr}(V_\mu V^\mu))^2 + \frac{1}{4}\varsigma_2\mathrm{Tr}(V_\mu V^\mu)S_\mu S^\mu \\ &+ \frac{1}{\sqrt{6}}\varsigma_3\mathrm{Tr}(V_\mu V^\mu V_\nu)S^\nu + \cdots + \delta\mathcal{L}_{M_2}^{SB} \ .\end{aligned} \tag{20}$$

The part $\delta\mathcal{L}_{M_2}^{SB}$ contains additional symmetry breaking terms with three and four meson fields and will be discussed in Section IV. The list of terms in Eq. (20) is not complete. The ellipsis stands for additional terms with four octet fields and terms which involve gradients of the meson fields. The gradient terms can be disregarded in the discussion of nuclear matter. Furthermore, only the time-like component of the meson mean fields is nonvanishing and the omitted contributions involving four octet fields can be reduced to the given terms.

III. THE MEAN FIELD APPROXIMATION

A. The loop expansion

In the following we will disregard weak decays and small isospin violations. We consider nuclear matter as a system with conserved baryon number (N_B), isospin (T_3) and strangeness (S). The corresponding chemical potentials are introduced by adding to the effective Lagrangian in Eq. (9) the contribution

$$\mu_B \mathrm{Tr}(\overline{B}\gamma^0 B) + \mu_3 \mathrm{Tr}\Big(\overline{B}\gamma^0 [T_3, B]\Big) + \mu_S \mathrm{Tr}\Big(\overline{B}\gamma^0 (B - [Y, B])\Big) \ , \tag{21}$$

where $S = N_B - Y$ was used. The isospin and hypercharge operator are expressed in terms of Gell-Mann matrices

$$T_3 = \frac{1}{2}\lambda_3 \quad , \quad Y = \frac{1}{\sqrt{3}}\lambda_8 \ . \tag{22}$$

The mean-field approximation follows from the the one-loop contribution to the thermodynamic potential. For the main parts the derivation is straightforward [33] and we will only briefly sketch the steps. Starting point for the loop expansion is the effective Lagrangian in Eq. (9) with all the meson field operators shifted by their expectation values:

$$\begin{aligned} \hat{\Pi} \to \hat{\Pi} + \Pi \quad , \quad \hat{V}_\mu \to \hat{V}_\mu + V_\mu \ , \\ \hat{S}_\mu \to \hat{S}_\mu + S_\mu \quad \text{and} \quad \hat{\varphi} \to \hat{\varphi} + \varphi \ , \end{aligned}$$

where the field operators are denoted with a hat. The symmetries of infinite nuclear matter simplify the discussion considerably. Translation and rotational invariance demand that the expectation values, or mean fields, of all three-vector fields vanish. The mean fields of the Goldstone bosons vanish because the nuclear matter ground state is assumed to have good parity. Finally, since the third component of the isospin and the total strangeness is fixed via the corresponding chemical potentials, $SU(3)$ symmetry demands that only the time-like components of the neutral vector mesons have a nonvanishing expectation value. At the one-loop level the thermodynamic potential is then obtained by diagonalizing

$$\begin{aligned} \mathcal{L}^{[1]} = \mathrm{Tr}\bigg(\overline{B}\Big(i\partial\!\!\!/ B + \mu_B\gamma^0 B + \mu_3\gamma^0[T_3, B] + \mu_S\gamma^0(B - [Y, B])\Big)\bigg) \\ - g_F \mathrm{Tr}\Big(\overline{B}\gamma^0[V_0, B]\Big) - g_D \mathrm{Tr}\Big(\overline{B}\gamma^0\{V_0, B\}\Big) - g_S \mathrm{Tr}\Big(\overline{B}\gamma^0 S_0 B\Big) \\ - \overline{N}(M_N - g_N^s\varphi)N - \overline{\Lambda}(M_\Lambda - g_\Lambda^s\varphi)\Lambda - \overline{\mathbf{\Sigma}}(M_\Sigma - g_\Sigma^s\varphi)\mathbf{\Sigma} - \overline{\Xi}(M_\Xi - g_\Xi^s\varphi)\Xi \\ + \frac{1}{2}m_\omega^2\omega_0^2 + \frac{1}{2}m_\phi^2\phi_0^2 + \frac{1}{2}m_\rho^2\rho_0^2 - \frac{1}{2}m_s^2\varphi^2 + \mathcal{V}(\varphi, \omega_0, \phi_0, \rho_0) \ , \end{aligned} \tag{23}$$

with

$$V_0 = \begin{pmatrix} \frac{\rho_0}{\sqrt{2}} + \frac{V_0^8}{\sqrt{6}} & 0 & 0 \\ 0 & \frac{V_0^8}{\sqrt{6}} - \frac{\rho_0}{\sqrt{2}} & 0 \\ 0 & 0 & -\frac{2}{\sqrt{6}}V_0^8 \end{pmatrix} \ . \tag{24}$$

The corresponding mean fields for the ω and ϕ arise from the mixing relation Eq. (8)

$$\begin{aligned} \omega_0 &= \cos(\theta) S_0 + \sin(\theta) V_0^8 \ , \\ \phi_0 &= \sin(\theta) S_0 - \cos(\theta) V_0^8 \ . \end{aligned} \tag{25}$$

The Lagrangian $\mathcal{L}^{[1]}$ is diagonal in flavor space except for a term which mixes the Λ and Σ^0. For the pure flavors the calculation is straightforward and the thermodynamic potential can be written as

$$\begin{aligned} \frac{\Omega}{V}(\mu_B, \mu_3, \mu_S) = &\frac{\Omega_p}{V} + \frac{\Omega_n}{V} + \frac{\Omega_{\Sigma^+}}{V} + \frac{\Omega_{\Sigma^-}}{V} + \frac{\Omega_{\Xi^0}}{V} + \frac{\Omega_{\Xi^-}}{V} + \frac{\Omega_{\Lambda\Sigma^0}}{V} \\ &- \frac{1}{2} m_\omega^2 \omega_0^2 - \frac{1}{2} m_\phi^2 \phi_0^2 - \frac{1}{2} m_\rho^2 \rho_0^2 + \frac{1}{2} m_s^2 \varphi^2 - \mathcal{V}(\varphi, \omega_0, \phi_0, \rho_0) \ . \end{aligned} \tag{26}$$

The one-body contribution can be divided into an explicit density dependent part and a divergent vacuum part

$$\frac{\Omega_F}{V} = \omega_F^0 + \omega_F^{vac} \tag{27}$$

with

$$\omega_F^0 = -\frac{1}{3\pi^2} \int_{M_F^*}^{\nu_F} dE (E^2 - {M_F^*}^2)^{3/2} \ , \tag{28}$$

and

$$\omega_F^{vac} = \frac{1}{2\pi^2} \frac{\Gamma(2 - \frac{D}{2})}{D(D-2)} \left({M_F^*}^4 \Big[\frac{{M_F^*}^2}{4\pi\lambda^2} \Big]^{D/2-2} - M_F^4 \Big[\frac{M_F^2}{4\pi\lambda^2} \Big]^{D/2-2} \right) \ . \tag{29}$$

The effective chemical potentials and the effective mass for each individual flavor are listed in Table I. The vacuum contribution includes a vacuum subtraction and was calculated in dimensional regularization which introduces the mass parameter λ. Before we discuss Eq. (26) further let us turn to the contribution of the Λ and Σ^0 which is more complicated due to the flavor mixing.

B. $\Lambda - \Sigma^0$ flavor mixing

Flavor mixing results from the nondiagonal part of the one-loop Lagrangian Eq. (23)

$$\begin{aligned} \mathcal{L}^{[1]}_{\Lambda\Sigma^0} = &\overline{\Psi}_\Lambda (i\partial\!\!\!/ - \gamma^0 V_\Lambda^0 - M_\Lambda^*) \Psi_\Lambda + \overline{\Psi}_{\Sigma^0} (i\partial\!\!\!/ - \gamma^0 V_{\Sigma^0}^0 - M_\Sigma^*) \Psi_{\Sigma^0} \\ &- \overline{\Psi}_\Lambda \gamma^0 V_m^0 \Psi_{\Sigma^0} - \overline{\Psi}_{\Sigma^0} \gamma^0 V_m^0 \Psi_\Lambda \ , \end{aligned} \tag{30}$$

with

$$V_m^0 = g_{\Lambda\Sigma}^\rho \rho^0 \ , \tag{31}$$

and where the other potentials and effective masses are listed in Table I. At the one-loop level the mean fields are the baryon self energies arising from a resummation of tadpole

diagrams involving loops with one baryon propagator. Due to the coupling $g^{\rho}_{\Lambda\Sigma}$ the vector self energies are non-diagonal in the $\Lambda - \Sigma^0$ sector of flavor space.

The Lagrangian Eq. (30) leads to a system of coupled Dirac equations

$$(i\partial\!\!\!/ - \gamma^0 V^0_\Lambda - M^*_\Lambda)\Psi_\Lambda = \gamma^0 V^0_m \Psi_{\Sigma^0} \ , \tag{32}$$

$$(i\partial\!\!\!/ - \gamma^0 V^0_{\Sigma^0} - M^*_\Sigma)\Psi_{\Sigma^0} = \gamma^0 V^0_m \Psi_\Lambda \ , \tag{33}$$

which has four energy eigenvalues corresponding to two particle and anti-particle solutions. Each flavor is then represented as a superposition of these two solutions. To be more specific let us consider the chiral limit $M^*_\Lambda = M^*_\Sigma \equiv M^*$. In this case the algebraic structure simplifies considerably and the Lagrangian Eq.(30) can be fully diagonalized by substituting for the fields

$$\Psi_\Lambda = \cos(\alpha)\Psi_1 + \sin(\alpha)\Psi_2 \tag{34}$$

$$\Psi_{\Sigma^0} = -\sin(\alpha)\Psi_1 + \cos(\alpha)\Psi_2 \tag{35}$$

$$\mathcal{L}^{[1]}_{\Lambda\Sigma^0} = \overline{\Psi}_1(i\partial\!\!\!/ - \gamma^0 V^0_1 - M^*)\Psi_1 + \overline{\Psi}_2(i\partial\!\!\!/ - \gamma^0 V^0_2 - M^*)\Psi_2 \ . \tag{36}$$

The mixing angle is determined by

$$\tan^2(\alpha) - \left(\frac{V^0_\Lambda - V^0_{\Sigma^0}}{V^0_m}\right)\tan(\alpha) - 1 = 0 \ , \tag{37}$$

and the potentials are given by

$$V^0_1 = \cos^2(\alpha)V^0_\Lambda + \sin^2(\alpha)V^0_{\Sigma^0} - 2\sin(\alpha)\cos(\alpha)V^0_m \ , \tag{38}$$

$$V^0_2 = \sin^2(\alpha)V^0_\Lambda + \cos^2(\alpha)V^0_{\Sigma^0} + 2\sin(\alpha)\cos(\alpha)V^0_m \ . \tag{39}$$

By using plane wave solutions for the corresponding Dirac equation the energy eigenvalues for particle 1 and 2 are now straightforward

$$E^\pm_1 = V^0_1 \pm \sqrt{\underline{p}^2 + M^{*2}} \quad , \quad E^\pm_2 = V^0_2 \pm \sqrt{\underline{p}^2 + M^{*2}} \ . \tag{40}$$

The $\Lambda - \Sigma^0$ mixing is related to the phenomenon of neutrino flavor mixing which gives rise to the recently much discussed neutrino oscillations. However, the origin of both effects is fundamentally different. Neutrino oscillations are assumed to occur in the vacuum arising from a nondiagonal mass matrix in flavor space which contains the vacuum mass parameters [22]. This effect can be appreciably enhanced when neutrinos pass through dense matter as predicted by the MSW effect [34]. In this case the mixing transformation which corresponds to Eqs. (34) and (35) induces a nontrivial vacuum structure with two unitary inequivalent vacuum states corresponding to the flavor and mass representation [35]. In contrast, the $\Lambda - \Sigma^0$ mixing is a *true many body effect* arising from a nondiagonal vector self energy which is generated in the medium. As long as small isospin violations can be neglected, the vacuum self energies are diagonal in flavor space and the asymptotic states can be properly identified as the pure flavor states.

As a consequence of the mixing transformation in Eqs. (34) and (35) the individual flavor states arise as superpositions of the particles 1 and 2. This implies that the nuclear matter ground state is generally in a state of mixed flavor rather than in a state with distinct Λ and

Σ^0 particles. A (quasi) particle interpretation is only possible in terms of the actual mass eigenstates 1 and 2.

For the general case we could not find a unitary transformation which leaves the kinetic terms in Eq. (30) invariant and which decouples the Lagrangian in a form similar to Eq. (36). However, it is possible to solve the coupled Dirac equations Eqs. (32) and (33) and to compute the thermodynamic potential. This is most easily done in euclidean space by using a path integral representation. The thermodynamic potential is then given by the determinant of the (euclidean) Lagrangian in Eq. (30). We find

$$\frac{\Omega_{\Lambda\Sigma^0}}{V} = -2\int\frac{d^4p}{(2\pi)^4}\ln\Big(\big[(\tilde{p}^0+\mathrm{i}U_2^0)^2+\underline{p}^2+M_\Lambda^{*2}\big]\big[(\tilde{p}^0-\mathrm{i}U_2^0)^2+\underline{p}^2+M_\Sigma^{*2}\big] - V_m^{02}\big[2M_\Lambda^*M_\Sigma^*+2\underline{p}^2-V_m^{02}-2U_2^{02}-2\tilde{p}^{02}\big]\Big) - VEV \ , \tag{41}$$

where we have introduced

$$U_1^0+U_2^0=-\nu_\Lambda \quad , \quad U_1^0-U_2^0=-\nu_{\Sigma^0}$$
$$\tilde{p}^0 = p^0+\mathrm{i}U_1^0 \ ,$$

and where VEV represents a vacuum subtraction. The momentum integral in Eq. (41) is performed in euclidean space. The matter and vacuum contribution can be extracted by deforming the integration contour down to the real axis, *i.e.* by using

$$\int_{-\infty}^{\infty}\frac{dp_0}{2\pi}\ln[f(p_0-\mathrm{i}V)] = i\int_0^V\frac{dp_0}{2\pi}\ln\left[\frac{f(-\mathrm{i}p_0+\epsilon}{f(-\mathrm{i}p_0-\epsilon}\right]+\int_{-\infty}^{\infty}\frac{dp_0}{2\pi}\ln[f(p_0)] \ , \tag{42}$$

where we have assumed that $f(ip_0)$ is analytic off the real axis and that $V>0$. Applied to Eq. (41) this leads to

$$\frac{\Omega_{\Lambda\Sigma^0}}{V} = \omega^0_{\Lambda\Sigma^0}+\omega^{vac}_{\Lambda\Sigma^0} \ . \tag{43}$$

The density dependent part can be written as

$$\omega^0_{\Lambda\Sigma^0} = -2\sum_{i=1,2}\int\frac{d^3p}{(2\pi)^3}(U_1^0-E_i^+)\Theta(U_1^0-E_i^+) \ , \tag{44}$$

where E_i^+ are the eigenvalues of the particle solutions of the Dirac equations Eq. (32) and Eq. (33). These eigenvalues are the roots of a fourth order polynomial given by the argument of the logarithm in Eq. (41). The roots have no simple analytic expression but can be calculated numerically. Including the vacuum subtraction the vacuum part is given by

$$\omega^{vac}_{\Lambda\Sigma^0} = -2\int\frac{d^4p}{(2\pi)^4}\Big\{\ln\Big(\big[(p^0+\mathrm{i}U_2^0)^2+\underline{p}^2+M_\Lambda^{*2}\big]\big[(p^0-\mathrm{i}U_2^0)^2+\underline{p}^2+M_\Sigma^{*2}\big] - V_m^{02}\big[2M_\Lambda^*M_\Sigma^*+2\underline{p}^2-V_m^{02}-2U_2^{02}-2p^{02}\big]\Big) - \ln\Big(\big[(p^0+\underline{p}^2+{M_\Lambda}^2\big]\big[p^0+\underline{p}^2+{M_\Sigma}^2\big]\Big)\Big\} \ . \tag{45}$$

To study the vacuum contribution in more detail it is useful to separate the contribution which does not depend on the vector potentials

$$\omega^{vac}_{\Lambda\Sigma^0} = \omega_1 + \omega_2 \ , \tag{46}$$

with

$$\omega_1 = -2\int\frac{d^4p}{(2\pi)^4}\ln\left(\frac{[(p^0+\underline{p}^2+M_\Lambda^{*2}][p^0+\underline{p}^2+M_\Sigma^{*2}]}{[(p^0+\underline{p}^2+M_\Lambda{}^2][p^0+\underline{p}^2+M_\Sigma{}^2]}\right) \ , \tag{47}$$

and

$$\begin{aligned}\omega_2 = -2\int\frac{d^4p}{(2\pi)^4}\Bigg\{&\ln\Bigg([(p^0+\mathrm{i}U_2^0)^2+\underline{p}^2+M_\Lambda^{*2}][p^0-\mathrm{i}U_2^0)^2+\underline{p}^2+M_\Sigma^{*2}] \\ &- V_m^{02}[2M_\Lambda^*M_\Sigma^* + 2\underline{p}^2 - V_m^{02} - 2U_2^{02} - 2p^{02}]\Bigg) \\ &- \ln\Bigg([(p^0+\underline{p}^2+M_\Lambda^{*2}][p^0+\underline{p}^2+M_\Sigma^{*2}]\Bigg)\Bigg\} \ .\end{aligned} \tag{48}$$

The contribution ω_1 is identical to the result in Eq. (29) for the pure flavors. The second term Eq. (48) vanishes in the chiral limit $M_\Lambda^* = M_\Sigma^*$ and for $V_m = 0$. In the vacuum ω_2 generates the n-point functions of the vector mesons at zero four momentum. These functions are in general non-zero because the vector mesons couple to a non-conserved current. As a consequence transversality is lost. To extract the divergencies Eq.(48) can be expanded in powers of V_m^2. Only the first term in this expansion is divergent

$$\omega_2^{inf} = \frac{1}{8\pi^2}\Gamma(2-\frac{D}{2})V_m^2(M_\Lambda^*-M_\Sigma^*)^2 \ .$$

indicating a renormalization of the ρ-meson mass.

From the explicit form of the thermodynamic potential in Eq. (43) various densities can be calculated by taking partial derivatives. The baryon densities for the Λ and Σ^0 follow from

$$\rho_B^\Lambda = -\frac{1}{V}\frac{\partial\Omega_{\Lambda\Sigma^0}}{\partial\nu_\Lambda} \quad , \quad \rho_B^{\Sigma^0} = -\frac{1}{V}\frac{\partial\Omega_{\Lambda\Sigma^0}}{\partial\nu_{\Sigma^0}}. \tag{49}$$

The corresponding scalar densities are given by

$$\rho_s^\Lambda = \frac{1}{V}\frac{\partial\Omega_{\Lambda\Sigma^0}}{\partial M_\Lambda^*} \quad , \quad \rho_s^\Lambda = \frac{1}{V}\frac{\partial\Omega_{\Lambda\Sigma^0}}{\partial M_\Sigma^*} \ . \tag{50}$$

As a consequence of the flavor mixing the mixed $\Lambda-\Sigma^0$ baryon density is nonzero:

$$\rho_B^{\Lambda\Sigma^0} \equiv < G|\overline{\Psi}_\Lambda\gamma^0\Psi_\Sigma^0|G> + < G|\overline{\Psi}_\Sigma^0\gamma^0\Psi_\Lambda|G> = \frac{1}{V}\frac{\partial\Omega_{\Lambda\Sigma^0}}{\partial V_m} \ . \tag{51}$$

In the limit $M_\Lambda^* = M_\Sigma^* \equiv M^*$ the flavor densities can be related to the densities of the mass eigenstates by using the relations Eq. (34) and Eq. (35):

$$\rho_B^{\Lambda} = \cos^2(\alpha)\rho_B^1 + \sin^2(\alpha)\rho_B^2 \ , \tag{52}$$
$$\rho_B^{\Sigma^0} = \sin^2(\alpha)\rho_B^1 + \cos^2(\alpha)\rho_B^2 \ , \tag{53}$$
$$\rho_B^{\Lambda\Sigma^0} = -2\sin(\alpha)\cos(\alpha)(\rho_B^1 - \rho_B^2) \ , \tag{54}$$

with

$$\rho_B^i = \frac{1}{V}\frac{\partial\Omega_{\Lambda\Sigma^0}}{\partial V_i^0} \ . \tag{55}$$

Thus, the sum of particles 1 and 2 equals the number of Λ and Σ^0 flavors in the system

$$\rho_B^1 + \rho_B^2 = \rho_B^{\Lambda} + \rho_B^{\Sigma^0} \ . \tag{56}$$

It is important to note that this relation also holds in the genral case $M_\Lambda^* \neq M_\Sigma^*$.

C. The equation of state

Before we display the relations which determine the equation of state let us briefly discuss the role of the vacuum contribution. The divergencies can be eliminated by introducing suitable counterterms in the original Lagrangian Eq. (9). At the one-loop level the counterterms are a fourth-order polynomial in the scalar field and the ρ-meson field. In practice, however, an explicit calculation of the counterterms is unnecessary. This is based on the observation that the vacuum contribution can be expanded in powers of the meson mean-fields. The original Lagrangian contains only terms of the order $\nu = 4$ and it is therefore consistent to truncate the expansion at fourth order. The truncated vacuum part can then be combined with the tree level contributions by redefining the coefficients of the nonlinear potential $\mathcal{V}$ in Eq. (20), *i.e.*

$$\frac{\Omega_{vac}}{V} - \delta\mathcal{L}_{CTC} - \mathcal{V} \to -\mathcal{V}' \ .$$

The details of how these coefficients arise in the formalism are unimportant because at the end of the calculation the coefficients are determined by fits to nuclear observables.

The actual mean-field configuration is determined by extremization of Eq. (26) at fixed chemical potentials. This leads to the self-consistency equations

$$m_\omega^2\omega_0 + \frac{\partial\mathcal{V}}{\partial\omega_0} = g_N^\omega(\rho_B^p + \rho_B^n) + g_\Lambda^\omega\rho_B^\Lambda + g_\Sigma^\omega(\rho_B^{\Sigma^0} + \rho_B^{\Sigma^-} + \rho_B^{\Sigma^+}) + g_\Xi^\omega(\rho_B^{\Xi^0} + \rho_B^{\Xi^-}) \ , \tag{57}$$
$$m_\rho^2\rho_0 + \frac{\partial\mathcal{V}}{\partial\rho_0} = \frac{1}{2}g_N^\rho(\rho_B^p - \rho_B^n) + g_\Sigma^\rho(\rho_B^{\Sigma^+} - \rho_B^{\Sigma^-}) + \frac{1}{2}g_\Xi^\rho(\rho_B^{\Xi^0} - \rho_B^{\Xi^-}) + g_{\Lambda\Sigma}^\rho\rho_B^{\Lambda\Sigma^0} \ , \tag{58}$$
$$m_\phi^2\phi_0 + \frac{\partial\mathcal{V}}{\partial\phi_0} = g_N^\phi(\rho_B^p + \rho_B^n) + g_\Lambda^\phi\rho_B^\Lambda + g_\Sigma^\phi(\rho_B^{\Sigma^0} + \rho_B^{\Sigma^-} + \rho_B^{\Sigma^+}) + g_\Xi^\phi(\rho_B^{\Xi^0} + \rho_B^{\Xi^-}) \ , \tag{59}$$
$$m_s^2\varphi - \frac{\partial\mathcal{V}}{\partial\varphi} = g_N^s(\rho_s^p + \rho_s^n) + g_\Lambda^s\rho_s^\Lambda + g_\Sigma^s(\rho_s^{\Sigma^0} + \rho_s^{\Sigma^-} + \rho_s^{\Sigma^+}) + g_\Xi^s(\rho_s^{\Xi^0} + \rho_s^{\Xi^-}) \ . \tag{60}$$

For the pure flavors the densities on the right hand side are defined by:

$$\rho_B^F = \frac{1}{3\pi^2}(\nu_F^2 - M_F^{*\,2})^{3/2} \ , \tag{61}$$

for the baryon densities and

$$\rho_s^F = \frac{M_F^*}{\pi^2}\int_{M_F^*}^{\nu_F} dE(E^2 - M_F^{*\,2})^{1/2} \ , \tag{62}$$

for the scalar densities. For the Λ and Σ^0 the corresponding quantities are listed in Section III B in Eqs. (49)-(51). Note that the ρ-meson couples to the mixed density $\rho_B^{\Lambda\Sigma^0}$ which enters the right hand side of Eq. (58). The self-consistency equations Eqs. (57)-(60) together with the expression for the thermodynamic potential Eq. (26) allows the computation of all thermodynamic quantities. For example, the energy density follows from the thermodynamic relation

$$\mathcal{E} = \frac{\Omega}{V} + \mu_B\rho_B + \mu_3\rho_3 + \mu_S\rho_S \ , \tag{63}$$

with the total baryon density

$$\rho_B = \sum_F \rho_B^F \ , \tag{64}$$

the total isospin density

$$\rho_B^3 = \sum_F t_3^F \rho_B^F \ , \tag{65}$$

and the total strangeness density

$$\rho_B^S = \sum_F s^F \rho_B^F \ , \tag{66}$$

where t_3^F was introduced for the isospin and s^F for the strangeness characterizing each flavor.

IV. MODEL PARAMETERS

Although a Lagrangian is at the heart of the effective hadronic field theory, an expansion in powers of the mean fields is a low density expansion, and neglecting many-body effects and loops involving the Goldstone bosons is hard to justify. The success of relativistic mean-field models can be understood in the context of density functional theory [36]. Central object is an energy functional of scalar and vector densities. Extremization of the functional gives rise to Dirac equations for the baryons with local scalar and vector potentials, not only at the one-loop level, but in the general case as well. In the so-called Kohn-Sham [37] approach to density functional theory one introduces auxiliary variables corresponding to the local potentials. The exact energy functional has kinetic-energy and Hartree parts which correspond to the one-loop contributions derived in section III, plus an exchange-correlation functional which contains all the complicated many-body effects. Formally, the solution of the many-body problem can be cast into solving the noninteracting problem of baryons moving in the local Kohn-Sham potentials. The resulting Dirac equations have the same

form as in a mean-field calculation, but correlation effects can be included if the proper exchange-correlation functional can be found. In the effective hadronic theory the meson mean fields play the role of Kohn-Sham potentials and by introducing nonlinear meson-meson couplings one can implicitly include additional density dependence. Thus, rather than try to construct an energy functional from an underlying Lagrangian, the basic idea is to approximate the functional using an expansion in terms of the meson mean fields [38,39]. If the parameters can be fit to nuclear observables, complicated many-body effects arising from loops will be incorporated.

Guided by these general remarks we will now specify the parameters contained in the basic Lagrangian Eq. (9). The baryon and vector meson masses are taken to have their experimental values which are listed in Table II. The assumption of $SU(3)$ symmetry implies that the couplings of the vector mesons to the baryons are characterized by four parameters: the octet couplings g_F, g_D, the singlet coupling g_S and the mixing angle θ which relates the physical vector mesons to their pure octet and singlet counterparts. The corresponding relations are listed in Table III. For the mixing angle we used the empirical value $\theta \simeq 37.2^\circ$ [40]. The parameters g_F, g_D and g_S were chosen to reproduce the values for the $NN\omega$ and $NN\rho$ couplings which have been obtained in Ref. [17] based on an effective field theory for ordinary nuclei. As a third constraint the OZI rule is implemented by requiring that the nucleon coupling to the ϕ meson vanishes. The couplings of the other baryons then follow from the $SU(3)$ relations in Table III.

In the scalar sector only the scalar coupling of the nucleon and the mass of the scalar meson have been determined within the framework of effective field theory [17]. In principle, the scalar coupling of the Λ has to be constraint to reproduce properties of hypernuclei. Such work has been reported in Ref. [20], however, their couplings cannot be used in our framework because the fits were based on a model which includes a very restricted subset of nonlinear meson-meson interactions. We therefore resort to a more phenomenological approach [10] which will also lead to an estimate for the corresponding couplings of the Σ and Ξ hyperons. There is a considerable amount of data available on binding energies and single particle levels of Λ hypernuclei [1] which are successfully described in various mean-field models. The key observation is that different models predict values for the potential felt by a single Λ in nuclear matter within a fairly narrow range [26,27]:

$$U_\Lambda = g^s_\Lambda \varphi - g^\omega_\Lambda \omega^0 \approx 27 - 28 \ (27.5)\text{MeV} \ . \tag{67}$$

Although the experimental status on Σ hypernuclei is still controversial, studies of level shifts and widths of Σ^- atoms suggest [41]

$$U_\Sigma = g^s_\Sigma \varphi - g^\omega_\Sigma \omega^0 \approx 20 - 30 \ (25)\text{MeV} \ . \tag{68}$$

The few events which have been attributed to the formation of a Ξ^--hypernucleus can be interpreted in terms of a potential [42]

$$U_\Xi = g^s_\Xi \varphi - g^\omega_\Xi \omega^0 \approx 20 - 25 \ (22.5)\text{MeV} \ . \tag{69}$$

The mean fields ω^0 and φ entering the potentials are taken at nuclear matter equilibrium and depend only on the nucleon couplings. Thus, the hyperon scalar couplings are completely determined by Eqs. (67)-(69). For the actual calibration the values in brackets were used.

Let us now turn to the nonlinear meson-meson couplings which are collected in the nonlinear potential $\mathcal{V} = \mathcal{V}(\varphi, \omega_0, \phi_0, \rho_0)$. In the effective field theory for normal nuclei ($\phi_0 = 0$) this potential was determined in a form [17]

$$\begin{aligned}\mathcal{V}(\varphi, \omega_0, \phi_0 = 0, \rho_0) = &-\frac{1}{3!}\kappa_3\varphi^3 - \frac{1}{4!}\kappa_4\varphi^4 \\ &+ \frac{1}{2}(\eta_\omega^1\varphi + \frac{1}{2}\eta_\omega^2\varphi^2)\omega_0^2 + \frac{1}{4!}\zeta_\omega\omega_0^4 + \frac{1}{2}\eta_\rho^1\varphi\rho_0^2 \ .\end{aligned} \tag{70}$$

The other allowed terms

$$\varphi^2\rho_0^2 \quad , \quad \omega^2\rho_0^2 \quad \text{and} \quad \rho_0^4 \ ,$$

can be expected to give negligible contributions in ordinary nuclei and were not included in the analysis. In our calibration procedure we require that the nonlinear potential in Eq. (20) reduces to the form given above for $\phi_0 = 0$. This determines nine parameters from the set

$$\{\kappa_3, \kappa_4, \eta_1^1, \eta_2^1, \eta_1^8, \eta_2^8, \zeta_1, \zeta_8, \varsigma_2, \varsigma_3\} \ .$$

We have arbitrarily chosen to let ς_3 undetermined. In the general case, ($\phi_0 \neq 0$), this procedure leads to predictions for the various couplings involving the ϕ meson based on $SU(3)$. Complications arise from terms which are linear in the ϕ meson mean field, *e.g.* terms of the form

$$\phi_0\,\omega_0^3 \quad , \quad \phi_0\,\varphi \quad \text{etc.}$$

These terms lead to abnormal, nonvanishing solutions for the mean field ϕ_0 if the total strangeness density of the system is zero. This is an indication that symmetry breaking terms are important for determining the nonlinear potential. The troublesome terms can be eliminated by constructing contributions which contain the quark mass matrix and combinations of three and four meson fields leading to a large number of new and unconstrained parameters. As a minimal approach we simply subtract the terms linear in the ϕ meson field. This leads to

$$\begin{aligned}\mathcal{V}(\varphi, \omega, \phi, \rho) = &\sum_{i,j,k,l=1}^{4} c_{i,j,k,l}\frac{1}{i!}\varphi^i\frac{1}{j!}\omega^j\frac{1}{k!}\phi^k\frac{1}{(2l)!}\rho^{2l} \\ &\text{with} \quad i+j+k+2l = 3,4 \quad \text{and} \quad k, 2l \geq 2 \ .\end{aligned} \tag{71}$$

Ultimately, the coefficients $c_{i,j,k,l}$ have to be constraint by properties of normal and hyper nuclei. The coefficients $c_{i,j,k,l}$ arise from a very large number of couplings in the original Lagrangian and are essentially independent. For nuclear structure calculations, however, it is not necessary to know how these coefficients arise. It is sufficient to know that the potential rewritten in terms of the physical meson fields is of the form given in Eq. (71).

The analysis of finite nuclei in Ref. [17] lead to two sets, G1 and G2, for the parameters $\{\kappa_3, \kappa_4, \eta_\omega^1, \eta_\omega^2, \zeta_\omega, \eta_\rho^1\}$ [1] which are listed together with the scalar mass and the nucleon-meson couplings in Table IV. The parameters were determined by calculating a set of

[1]The parameter sets G1 and G2 contain aditional parameters involving tensor couplings and meson-field gradients which are not needed in nuclear matter.

nuclear properties for a selected set of nuclei and by adjusting the parameters to minimize a generalized χ^2. Among others, the nuclear properties include binding energies, rms charge radii and spin-orbit splittings. In spite of the differences in the parameters the sets G1 and G2 yield similar properties of nuclear matter.

These sets G1 and G2 are the input in the calibration procedure as outlined above. The symmetry breaking parameter ς_3 which is not determined is set to zero. For the octet couplings we find $g_F/(g_F + g_D) = 0.97$ and $g_F/(g_F + g_D) = 0.95$ for the set G1 and G2 respectively, which is close to the *universality* value $g_F/(g_F + g_D) = 1$ [43]. To test whether the calibration procedure leads to reasonable values for the nonlinear coupling constants we have checked naturalness. A generic term of the potential can be written as

$$c_{i,j,k,l}\frac{1}{i!}\varphi^i\frac{1}{j!}\omega^j\frac{1}{k!}\phi^k\frac{1}{(2l)!}\rho^{2l} = g\frac{1}{i!}\left(\frac{\varphi}{f_\pi}\right)^i\frac{1}{j!}\left(\frac{\omega_0}{f_\pi}\right)^j\frac{1}{k!}\left(\frac{\phi_0}{f_\pi}\right)^k\frac{1}{(2l)!}\left(\frac{\rho_0}{f_\pi}\right)^{2l} f_\pi^2 M_N^2 \ . \qquad (72)$$

The overall coupling g is dimensionless and of $\mathcal{O}(1)$ if naturalness holds. For normal nuclei it has been demonstrated that the parameter set G1 and G2 are natural [17]. We found that the additional parameters which contain the ϕ meson field are also of $\mathcal{O}(1)$ and that our calibration procedure gives (at least) a natural set of coupling constants.

V. STRANGE NUCLEAR MATTER

We consider nuclear matter as a simple model for multi-strange systems which might be created during the evaporation process following central collisions of very heavy ions [11]. We assume that the time scale during which the system is observed is small enough so that the weak decays of the strange baryons can be neglected. The system is then characterized by the overall strangeness and isospin. To be specific we introduce the ratios

$$x_3 \equiv \frac{T_3}{N_B} = \frac{\rho_B^3}{\rho_B} \quad \text{and} \quad x_S \equiv \frac{S}{N_B} = \frac{\rho_B^S}{\rho_B} \qquad (73)$$

where the densities were introduced at the end of sect. 4, and assume that the isospin and strangeness ratio is held constant. Typical values for the isospin ratio in normal and hypernuclei are $|x_3| \lesssim 0.11$. Strangeness ratios in heavy hypernuclei are very small but values up to $x_S \simeq 1/3$ have been observed in light single and double hypernuclei [1]. Theoretically, metastable multi-strange systems have been predicted with strangeness ratios exceeding $x_S = 1$ [10].

At this point some caveats must be added. Our discussion of the theory will encompass a wide range of x_3 and x_S and we will extrapolate to regimes of high densities to obtain estimates for the empirical size of the new effects. The model was calibrated by using information of normal nuclei and single hypernuclei. Terms which have been neglected or which cannot be calibrated accurately, *i.e.*, nonlinear couplings involving the ρ and ϕ meson, are likely to be more important in systems with large isospin and strangeness ratios than in ordinary nuclei and single hypernuclei. Furthermore, the effective field theory is designed for calculations at low and moderate nuclear densities. It is unclear how far the truncated theory can be extrapolated to high densities. We will leave these problems aside in the following and focus on the new effects arising from the flavor mixing.

Nuclear matter is bound over a wide range of x_3 and x_S. This can be deduced from Fig. 1, where the binding energy is shown as a function of the baryon density. In part (a) we consider curves for various strangeness ratios at fixed isospin. At low and moderate densities an increase of the strangeness leads to higher energies. At high densities one observes the opposite trend; the curves become significantly softer for higher values of x_S. Part (b) of Fig. 1 indicates binding energies for various isospin ratios at fixed x_S. Increasing the overall isospin always adds more repulsion to the system. The origin of this behavior is mainly a Fermi gas effect. The main contribution to the energy in Fig. 1 comes from the nonstrange baryons. Increasing the strangeness increases the fraction of the strange baryons leading to more symmetric systems with smaller energies. If the absolute value of the isospin increases the fraction of certain flavors increases leading to more asymmetric systems with higher energies.

Typical flavor fractions are depicted in Fig. 2. In addition to the nucleons the Λ and Σ^0 fractions are nonzero at all densities for $x_S > 0$ and $x_3 \neq 0$. The onset of the other flavors is determined by the condition

$$\nu_F > M_F^* \ . \tag{74}$$

The properties of the Λ and Σ^0 is governed by the flavor mixing. The effect is driven by the mean field of the ρ meson and does not occur in isospin saturated systems ($x_3 = 0$). As the lightest hyperon the Λ is expected to give the main contribution of the strange baryons at low densities. Remarkably, the baryon density of the Σ^0 is *nonzero* even if the condition Eq. (74) is not fulfilled. This is because the nuclear matter ground state is not a state filled with distinct Λ and Σ^0 flavors rather than a state filled with the mass eigenstates 1 and 2 of the Dirac equations Eqs. (32) and (33).

The situation is illustrated in Fig. 3. The lower half of part (a) indicates the contributions of the mass eigenstates 1 and 2 to the thermodynamic potential according to Eq. (44). The labels are chosen such that solution 1 reduces to the Λ and solution 2 to the Σ^0 in the limit $V_m = 0$. Below the density ρ_B^2 only solution 1 gives a contribution. The mass eigenstate 1 consists mainly of the Λ flavor with a small admixture of the Σ^0 leading to nonzero Σ^0 density fraction in this region. It increases more rapidly when the second mass eigenstate emerges at ρ_B^2. The system in part (b) of Fig. 3 has the same strangeness ratio as in part (a) but $x_3 = 0$. As a consequence the mixing vanishes ($V_m = 0$). The lower half now indicates the thermodynamic potentials of pure Λ and Σ^0 flavors. The onset of the Σ^0 is governed by Eq. (74) which is not fulfilled for $\rho_B < \rho_B^{2\prime}$. The density and the contribution to the thermodynamic potential of the Σ^0 vanish in this region.

The onset of the pure strange flavors depends strongly on the overall isospin and strangeness content of the system as indicated in Fig. 4 for the $\Sigma^\pm$ and $\Xi^{\overline{0}}$. Decreasing x_3 delays the onset of the Σ^+ and Ξ^0. For sufficiently small values of x_3 these two flavors disappear altogether.

Another signature of $\Lambda - \Sigma^0$ flavor mixing is a nonvanishing value of the mixing density Eq. (51). At high densities the mixing density is comparable to the baryon densities of the strange flavors as indicated in Fig. 2. The effect is stronger if either the overall isospin or the strangeness is increased. This can be studied in Fig. 5, which shows the mixing density for various isospin and strangeness ratios. The kinks at low densities are caused by the onset of the Ξ^-. At low and moderate densities, the mixing density is very small.

Generally, we observe a strong parameter dependence. First, the coupling $g^{\rho}_{\Lambda\Sigma}$ and therefore the flavor mixing is smaller for the set G1. Second, in the high density regime the set G1 and G2 predict significant different flavor fractions. This is a common observation in relativistic mean field models. Different models and parametrizations which are equivalent at low and moderate densities can produce significantly different results when extrapolated to regimes of high densities [38].

VI. NEUTRON STAR MATTER

In this section we apply our model to describe dense matter in neutron stars. Recently, the study of strangeness in dense matter has received considerable attention due to the possibility of kaon condensation [13]. However, the question of kaon condensation is quite delicate and very sensitive to the employed parameters and models [15,16]. It is therefore important to study all the relevant many-body effects which have impact on the equation of state.

Throughout the last section we assumed that the time scales are sufficiently short such that weak processes can be neglected. As a model for cold neutron star matter we consider baryons, electrons and muons in chemical equilibrium with respect to weak decays [44]. This is equivalent to introducing two chemical potentials characterizing the conservation of baryon number and electric charge. This situation is realized by adding contributions of free, relativistic electrons and muons to the baryonic equation of state. The chemical potential for the electric charge is introduced by adding

$$\mu_q J^0_Q = \mu_q (J^0_{BQ} - \overline{\Psi}_e \gamma^0 \Psi_e - \overline{\Psi}_\mu \gamma^0 \Psi_\mu) \ , \tag{75}$$

to the effective Lagrangian in Eq. (9). The charge density of the baryons is given by

$$J^0_{BQ} = \mathrm{Tr}\Big(\overline{B}\gamma^0 [Q, B]\Big) \ , \tag{76}$$

where the charge matrix is given in terms the isospin and hypercharge operator by

$$Q = \frac{1}{2} Y + T_3 \ . \tag{77}$$

Overall charge neutrality is achieved by imposing

$$< G | J^0_{BQ} - \overline{\Psi}_e \gamma^0 \Psi_e - \overline{\Psi}_\mu \gamma^0 \Psi_\mu | G >= 0 \ , \tag{78}$$

on the ground-state expectation value of the charge density. The resulting equation of state for the two parameter sets G1 and G2 are shown in Fig. 6. At low and moderate densities the two parameter sets are essentially equivalent. At higher densities the set G2 produces a significantly softer equation of state.

The corresponding density fractions are indicated in Fig. 7. At low densities the proton fraction is very small and the system resembles pure neutron matter. At $\rho_B/\rho^0_B \approx 0.75$ the muons start to emerge. The first strange baryon, the Σ^-, starts at $\rho_B/\rho^0_B \approx 2$ followed closely by the Λ. Due to the flavor mixing there is also a small fraction of the Σ^0. The onset of the Ξ^- is at $\rho_B/\rho^0_B \approx 4.5$. As the last flavor, the Σ^+ emerges at $\rho_B/\rho^0_B \approx 7.5$. The fraction

of the Σ^0 becomes noticeable around $\rho_B/\rho_B^0 \approx 5.5$ where the second mass eigenstate starts to contribute to the equation of state as indicated by the black dot. In the usual scenario [16,44] without the flavor mixing the Σ^0 would not be present in the system below this point. Also included in Fig. 6 is the mixing density. At high densities its size is comparable to the other strange flavors indicating strong flavor mixing. A more quantitative estimate of the flavor mixing at low densities can be obtained from Fig. 8. Similar as in the previous figure, the onset of the second mass eigenstate is indicated by the black dots. Below that point the sum of the flavor densities equals the density of state 1, according to Eq. (56). It mainly consists of the Λ flavor, the admixture of the Σ^0 is very small ($\lesssim 0.1\%$).

VII. FLAVOR OSCILLATIONS

As discussed in section III B the Λ and Σ^0 flavor eigenstates are not the mass or energy eigenstates of the Lagrangian in Eq. (30) rather than a superposition of the actual mass eigenstates. The true, time independent nuclear matter ground state arises as a state filled with particles corresponding to the mass eigenstates. Adding a distinct flavor to the ground state creates a perturbation which evolves nontrivially in time leading to flavor oscillations. To study this phenomenon in more detail we will restrict our considerations to the limit $M_\Lambda^* = M_\Sigma^* \equiv M^*$. In this case the algebraic structure simplifies considerably allowing us to give explicit analytic expressions yet preserving the main physical content.

According to section III B the general solution of the Dirac equations Eqs. (32) and (33) which uncouples the Lagrangian Eq. (30) can be written as

$$\Psi_\Lambda = \cos(\alpha)\Psi_1 + \sin(\alpha)\Psi_2 \ , \tag{79}$$

$$\Psi_{\Sigma^0} = -\sin(\alpha)\Psi_1 + \cos(\alpha)\Psi_2 \ . \tag{80}$$

The fields Ψ_1 and Ψ_2 describe the normal modes which can be quantized canonically [45]:

$$\Psi_i(x) = e^{-iV_i^0 x_0} \int \frac{d^3p}{(2\pi)^3} \frac{M^*}{E} \sum_{s=1,2} \left(b_s^i(p) u^{(s)}(p) e^{-ipx} + d_s^{i\,\dagger}(p) v^{(s)}(p) e^{ipx} \right) , \tag{81}$$

with $E = \sqrt{\underline{p}^2 + M^{*2}}$ and with the potentials V_i^0 introduced in Eqs. (38) and (39). The operators b_s^i and d_s^i satisfy the usual anti-commutation relations. In the mean field approximation the nuclear matter ground state $|G>$ contains positive-energy levels of particles 1 and 2 filled to the chemical potentials (Fermi energies)

$$\mu_1 = \cos^2(\alpha)\mu_\Lambda + \sin^2(\alpha)\mu_{\Sigma^0} \ , \tag{82}$$

$$\mu_2 = \sin^2(\alpha)\mu_\Lambda + \cos^2(\alpha)\mu_{\Sigma^0} \ . \tag{83}$$

A state of flavor Λ with momentum $\underline{p}$ and spin s relative to the ground state can be constructed by adding a particle 1 and 2 above the Fermi energies

$$|\varphi_\Lambda(\underline{p}, s)> = \Big(\cos(\alpha) b_s^{1\,\dagger}(p) + \sin(\alpha) b_s^{2\,\dagger}(p)\Big)|G> \quad \text{with} \quad E + V_i^0 > \mu_i \ . \tag{84}$$

The normalization is chosen such that at $x_0 = 0$

$$\int_V d^3x < \varphi_\Lambda(\underline{p},s)|\overline{\Psi}_\Lambda\gamma^0\Psi_\Lambda|\varphi_\Lambda(\underline{k},s') > \; = (2\pi)^3\frac{E}{M^*}\delta_{ss'}\delta^{(3)}(\underline{p}-\underline{k})(1+N_G^\Lambda)\;, \tag{85}$$

$$\int_V d^3x < \varphi_\Lambda(\underline{p},s)|\overline{\Psi}_{\Sigma^0}\gamma^0\Psi_{\Sigma^0}|\varphi_\Lambda(\underline{k},s') > \; = (2\pi)^3\frac{E}{M^*}\delta_{ss'}\delta^{(3)}(\underline{p}-\underline{k})N_G^{\Sigma^0}\;, \tag{86}$$

with

$$\int_V d^3x < G|\overline{\Psi}_\Lambda\gamma^0\Psi_\Lambda|G >= N_G^\Lambda \quad \text{and} \quad \int_V d^3x < G|\overline{\Psi}_{\Sigma^0}\gamma^0\Psi_{\Sigma^0}|G >= N_G^{\Sigma^0}\;,$$

for the number of Λ and Σ^0 in the ground state at $x_0 = 0$ [2]. At a later time $x_0 > 0$ the transition amplitude of finding the system in the Λ flavor state is given by

$$\begin{aligned}(2\pi)^3\delta_{ss'}\delta^{(3)}(\underline{p}-\underline{k})a_{\underline{p},s}^{\Lambda\Lambda} &= < \varphi_\Lambda(\underline{p},s)|e^{-ix_0H}|\varphi_\Lambda(\underline{k},s') > \\ &= (2\pi)^3\delta_{ss'}\delta^{(3)}(\underline{p}-\underline{k})\int\frac{dp_0}{2\pi}e^{-ip_0x_0}\overline{u}^{(s)}(p)\gamma^0G^{\Lambda\Lambda}(p)\gamma^0u^{(s)}(p)\;.\end{aligned} \tag{87}$$

The transition amplitude involves the $\Lambda\Lambda$-Greens function which can be computed by using the representation Eqs. (5) and (7) for the field operators [46]

$$\begin{aligned}G^{\Lambda\Lambda}(x-y) &= < G|T[\Psi_\Lambda(x)\overline{\Psi}_\Lambda(y)]|G > \\ &= \cos^2(\alpha) < G|T[\Psi_1(x)\overline{\Psi}_1(y)]|G > + \sin^2(\alpha) < G|T[\Psi_2(x)\overline{\Psi}_2(y)]|G > \\ &\equiv \cos^2(\alpha)G^1(x-y) + \sin^2(\alpha)G^2(x-y)\;.\end{aligned} \tag{88}$$

The momentum-space representation of the Greens function of particles 1 and 2 is [33]

$$G^i(p) = i\frac{\not{p}-\not{V}_i+M^*}{(p-V_i)^2-M^{*2}+i\epsilon} - \frac{\pi}{E}(\not{p}-\not{V}_i+M^*)\delta(p_0-V_i^0-E)\Theta(\mu_i-V_i^0-E)\;. \tag{89}$$

After performing the p_0 integration in Eq. (87) the transition probability of finding the system in the state $|\varphi_\Lambda(\underline{p},s) >$ at time x_0 follows to

$$\begin{aligned}P_{\underline{p},s}^{\Lambda\Lambda}(x_0) &= |a_{\underline{p},s}^{\Lambda\Lambda}|^2 \\ &= \frac{E^2}{M^{*2}}\Big(1-\sin^2(2\alpha)\sin^2\Big[\frac{(V_1^0-V_2^0)}{2}x_0\Big]\Big)\Theta(E+V_1^0-\mu_1)\Theta(E+V_2^0-\mu_2)\;.\end{aligned} \tag{90}$$

Similar as in Eq. (84) one can also define a Σ^0 state

$$|\varphi_{\Sigma^0}(\underline{p},s) >= \Big(\sin(\alpha)b_s^{1\dagger}(p) - \cos(\alpha)b_s^{2\dagger}(p)\Big)|G > \;\; . \tag{91}$$

The probability for a transition of the state $|\varphi_\Lambda >$ to the state $|\varphi_{\Sigma^0} >$ involves the *mixed* $\Lambda\Sigma^0$-Greens function. Repeating the steps which lead to Eq. (90), it becomes

$$P_{\underline{p},s}^{\Lambda\Sigma^0}(x_0) = \frac{E^2}{M^{*2}}\sin^2(2\alpha)\sin^2\Big[\frac{(V_1^0-V_2^0)}{2}x_0\Big]\Theta(E+V_1^0-\mu_1)\Theta(E+V_2^0-\mu_2)\;. \tag{92}$$

---

[2] We consider the system in a finite volume V and take the thermodynamic limit at the end of the calculation.

Thus the probabilities for finding the system in the Λ or Σ^0 flavor state oscillate with frequency

$$\omega_F = \frac{(V_1^0 - V_2^0)}{2} \ , \tag{93}$$

arising from the interference of particle 1 and 2. The nuclear matter ground state also offers the possibility to create Λ hole states by destroying a particle 1 and 2 below the Fermi energies

$$|\varphi_\Lambda^h(\underline{p},s) >= \Big(\cos(\alpha) b_s^1(p) + \sin(\alpha) b_s^2(p)\Big)|G > \quad \text{with} \quad E + V_i^0 < \mu_i \ . \tag{94}$$

The probability of finding the system in the Λ hole state at a later time x_0

$$P_{\underline{p},s}^{\Lambda^h\Lambda^h}(x_0) = \frac{E^2}{M^{*2}}\Big(1 - \sin^2(2\alpha)\sin^2\Big[\frac{(V_1^0 - V_2^0)}{2}x_0\Big]\Big)\Theta(\mu_1 - E - V_1^0)\Theta(\mu_2 - E - V_2^0) \ ,$$

is identical to the expression for $P^{\Lambda\Lambda}$ in Eq. (90) except for the arguments of the step functions.

The flavor oscillations are governed by the frequencies ω_F and by the factor $\sin(2\alpha)$. The system unmixes if $\sin(2\alpha) = 0$, maximal mixing occurs for $\sin(2\alpha) = 1$ which corresponds to $\sin(\alpha) = \cos(\alpha) = \sqrt{2}/2$. For neutron star matter these quantities are indicated in Fig. 9. The results were obtained by using $M^* = (M_\Lambda^* + M_\Sigma^*)/2$ [3]. The frequencies in the upper part of Fig. 9 steadily increase with increasing density. The factor $\sin(2\alpha)$ is shown in the lower part. The mixing angle in Eq. (37) is determined by the mean field of the ρ meson and by the difference $V_\Lambda^0 - V_{\Sigma^0}^0$. The mixing is large at low densities because here the matter is very neutron rich. The system becomes more symmetric with increasing density leading to smaller mixing angles. At the minimum ($\rho_B/\rho_B^0 \approx 2$) the Σ^- starts to emerge as the first strange baryon and the mixing angle increases again. According to our remarks at the end of Sec. V we observe a sizable parameter dependence. The set G2 predicts higher mixing frequencies and stronger mixing. To obtain an estimate for the size of the effect, the results in the lower part of Fig. 9 can be compared with the rather small value $\sin(2\alpha^{ud}) \approx 0.02$ characterizing the mixing in the vacuum induced by the mass difference of the up and down quarks [24]. Thus, in the medium flavor mixing is much larger than typical isospin violating effects and thus might be easier to observe.

VIII. SUMMARY

In this paper we study strange nuclear matter based on concepts of effective field theory. Our starting point is a chiral effective Lagrangian containing the baryon octet, the Goldstone boson octet, the vector meson octet and a light scalar singlet. Guiding principle are the underlying symmetries of QCD which, in principle, implies that an infinite number of interaction terms has to be considered. We truncate the effective theory based on the

[3] Numerically, this is in fact a good approximation for calculating the equation of state.

observation that at low and moderate densities the meson mean fields are small compared to the baryon masses and thus provide useful expansion parameters. We develop a mean field model based on the one-loop approximation of the thermodynamic potential. It contains the one-body contributions of the baryons and a nonlinear potential which is a fourth order polynomial in the meson mean fields. These fields are interpreted as relativistic Kohn-Sham potentials and nonlinear interactions between the meson fields parametrize density dependence which, in principle, is beyond the one-loop or mean field level. A necessary condition is that the model parameters can be accurately calibrated to observed properties of ordinary nuclei and hypernuclei.

In the nonstrange sector we use the coupling constants which have been obtained in an EFT description for normal nuclei [17]. The scalar hyperon couplings are determined by using phenomenological information on the hyperon potential in nuclear matter. However, the nonlinear meson-meson couplings involving the ϕ meson remain largely unconstrained.

In spite of this difficulty the EFT description leads to new and interesting effects. The most important observation is that the D-type coupling between baryons and vector mesons leads to a nondiagonal vector self-energy in the $\Lambda - \Sigma^0$ sector of flavor space. As a consequence $\Lambda - \Sigma^0$ flavor mixing arises. Our basic goal is to provide a first orientation of the formalism by studying nuclear matter. Although, the discussion in nuclear matter is an oversimplification we believe it is useful for providing a concrete description and for examining qualitative features of the flavor mixing. We discuss various nuclear matter systems with different isospin and strangeness content as a simple model for multi-strange systems. We find that nuclear matter is in a state of mixed flavor rather than in a state with distinct Λ and Σ^0 particles. This implies that systems which contain Λ hyperons always have a small admixture of Σ^0 hyperons. At low and moderate densities the features are small but we expect that signatures will survive in calculations of very heavy and asymmetric hypernuclei.

The model was then used to study dense matter in neutron stars. In the presence of strangeness the equation of state suffers considerably from model and parameter dependence. Particularly, predictions for the onset of kaon condensation depend sensitively on model features relating to the nucleon-hyperon and hyperon-hyperon interaction. It is therefore important to estimate the influence of all the relevant many-body effects on the high-density equation of state. We find qualitative new features for the occurrence of the individual flavors in a neutron star. Due to the flavor mixing the Λ and Σ^0 start to emerge at the same value of the baryon density in contrast to the usual scenarios were the onset of the Σ^0 is delayed.

Similar to the phenomenon of neutrino oscillations, the time independent ground state of nuclear matter responds to external perturbations with flavor oscillations characterized by distinct frequencies. In contrast to the neutrino oscillations which primarily occur in the vacuum the $\Lambda - \Sigma^0$ mixing is a true many-body effect and vanishes at zero baryon density. Moreover, mixing of the Λ and Σ^0 can also arise in the vacuum if isospin violating effects are taken into account, however, we find that the effect in the medium is considerably larger.

To summarize, concepts and methods of effective field theory which have been applied to ordinary nuclei can be extended to incorporate strangeness in nuclear structure. The complexity of the underlying $SU(3)$ symmetry leads to a large number of interaction terms which are not well constrained in the strange sector. To achieve more predictive power future studies are needed to determine the coupling constants by incorporating the presently

available information on single and double hypernuclei.

ACKNOWLEDGMENTS

We thank H. W. Hammer, J. N. Ng and H. M. Saldaña for useful comments. This work was supported by the Natural Science and Engineering Research Council of Canada.

REFERENCES

[1] H. Bandō, T. Motoba and J. Žofka, *Int. J. of Mod. Phys. A* 5 (1990) 4021.

[2] M. M. Nagels, T. A. Rijken and J. J. de Swart, Phys. Rev. D 17 (1978) 768.
P. M. M. Maessen, T. A. Rijken and J. J. de Swart, Phys. Rev. C 40 (1989) 2226.

[3] B. Holzenkamp, K. Holinde and J. Speth, Nucl. Phys. A 500 (1989) 485.
A. Reuber, K. Holinde, H.-C. Kim and J. Speth, Nucl. Phys. A 608 (1996) 243.

[4] M. Rayet, Nucl. Phys. A 367 (1981) 381.

[5] M. Rufa, H. Stöcker, J. Maruhn, W. Greiner, and P. -G. Reinhard, J. Phys. G 13 (1987) L143.
J. Mareš and J. Žofka, Z. Phys. A 333 (1989) 209.

[6] J. Schaffner, C. B. Dover, A. Gal, C. Greiner, and H. Stöcker, Phys. Rev. Lett. 71 (1993) 1328.

[7] P. Papazoglou, S. Schramm, J. Schaffner-Bielich, H.Stöcker and W. Greiner, Phys. Rev. C 57 (1998) 2576.

[8] P. Papazoglou, D. Zschiesche, S. Schramm, J. Schaffner-Bielich, H.Stöcker and W. Greiner, `nucl-th/9806087`.

[9] B. K. Jennings, Phys. Lett. B 246 (1990) 325.
E. D. Cooper, B. K. Jennings and J. Mareš, Nucl. Phys. A 580 (1994) 419.

[10] J. Schaffner, C. B. Dover, A. Gal, C. Greiner, D. J. Millener and H. Stöcker, Ann. Phys. (N.Y.) 235 (1994) 35.

[11] C. Greiner and J. Schaffner, *Int. J. of Mod. Phys. E* 5 (1996) 239.

[12] B. V. Danilin and A. A. Korsheninnikov, Sov. J. Nucl. Phys. 50 (1989) 975.

[13] D. B. Kaplan and A. E. Nelson, Phys. Lett. B 175 (1986) 57.
A. E. Nelson and D. B. Kaplan, Phys. Lett. B 192 (1987) 193.

[14] J. Ellis, J. I. Kapusta and K. A. Olive, Nucl. Phys. B 348 (1991) 345.

[15] R. Knorren, M. Prakash and P. J. Ellis, Phys. Rev. C 52 (1995) 3470.

[16] J. Schaffner and I. N. Mishustin, Phys. Rev. C 53 (1996) 1416.

[17] R. J. Furnstahl, B. D. Serot, and H.-B. Tang, Nucl. Phys. A 615 (1997) 441.

[18] B. D. Serot and J. D. Walecka, *Int. J. of Mod. Phys. E* 6 (1997) 515.

[19] H. Georgi, Phys. Lett. B 298 (1993) 187.

[20] M. Rufa, J. Schaffner, J. Maruhn, H. Stöcker, W. Greiner and P. -G. Reinhard, Phys. Rev. C 42 (1990) 2469.

[21] R. J. Furnstahl, H. -B. Tang and B. D. Serot, Phys. Rev. C 52 (1995) 1368.

[22] S. M. Bilenky and B. Pontecorvo, Phys. Rep. 41 (1978) 225.

[23] C. B. Dover, H. Feshbach and A. Gal, Phys. Rev. C 51 (1995) 541.

[24] J. Gasser and H. Leutwyler, Phys. Rep. 87 (1982) 77.

[25] R. H. Dalitz and F. von Hippel, Phys. Lett. 10 (1964) 153.

[26] D. J. Millner, C. B. Dover and A. Gal, Phys. Rev. C 38 (1988) 2700.

[27] D. E. Lanskoy and Y. Yamamoto, Phys. Rev. C 55 (1997) 2330.

[28] E. K. Heide, S. Rudaz and P. J. Ellis, Nucl. Phys. A 571 (1994) 713.

[29] M. C. Birse, J. Phys. G 20 (1994) 1287.

[30] G. Ecker, J. Gasser, A. Pich and E. De Rafael, Nucl. Phys. B321 (1989) 311.
G. Ecker, J. Gasser, H. Leutwyler and E. De Rafael, Phys. Lett. B 223 (1989) 425.

[31] C. G. Callan, Jr., S. Coleman, J. Wess and B. Zumino, Phys. Rev. 177 (1969) 2247.

[32] J. F. Donoghue, E. Golowich and B. R. Holstein, *Dynamics of the Standard Model*, (Cambridge Univ. Press, 1992).
[33] B. D. Serot, Rep. Prog. Phys. 55 (1992) 1855.
[34] L. Wolfenstein, Phys. Rev. D 17 (1978) 2369.
S. P. Mikheev and A. Yu. Smirnov, Sov. J. Nucl. Phys. 42 (1985) 913.
[35] M. Blasone and G. Vitiello, Ann. Phys. (N.Y.) 244 (1995) 283. [Erratum:Ann. Phys. (N.Y.) 249 (1996) 363]
[36] R. M. Dreizler and E. K. U. Gross, *Denity functional theory* (Springer 1990).
[37] W. Kohn and L. J. Sham, Phys. Rev. A 140 (1965) 1133.
[38] H. Müller and B. D. Serot, Nucl. Phys. A 606 (1996) 508.
[39] R. J. Furnstahl, B. D. Serot, and H.-B. Tang, Nucl. Phys. A 598 (1996) 539.
[40] E. Jenkins, A. V. Manohar and M. B. Wise, Phys. Rev. Lett. 75 (1995) 2272.
[41] C. B. Dover, D. J. Millner and A. Gal, Phys. Rep. 184 (1989) 1.
[42] C. B. Dover and A. Gal, Ann. Phys. (N.Y.) 146 (1983) 309.
[43] J. J. Sakurai, Ann. Phys. (N.Y.) 11 (1960) 1.
[44] N. K. Glendenning, Phys. Lett. B 114 (1982) 392.
[45] C. Itzykson and J.-B. Zuber, *Quantum Field Theory* (McGraw-Hill, 1980)
[46] M. Blasone, P. A. Henning and G. Vitiello, `hep-th/9803157`.

TABLES

TABLE I. Chemical potentials ($\nu_F = \mu_F - V_F^0$) and effective baryon masses.

F	μ_F	V_F^0	M_F^*
p	$\mu_B + \frac{1}{2}\mu_3$	$g_N^\omega \omega^0 + g_N^\phi \phi_0 + \frac{1}{2} g_N^\rho \rho_0$	$M_N - g_N^s \varphi$
n	$\mu_B - \frac{1}{2}\mu_3$	$g_N^\omega \omega^0 + g_N^\phi \phi_0 - \frac{1}{2} g_N^\rho \rho_0$	$M_N - g_N^s \varphi$
Λ	$\mu_B + \mu_S$	$g_\Lambda^\omega \omega^0 + g_\Lambda^\phi \phi_0$	$M_\Lambda - g_\Lambda^s \varphi$
Σ^0	$\mu_B + \mu_S$	$g_\Sigma^\omega \omega^0 + g_\Sigma^\phi \phi_0$	$M_N - g_\Sigma^s \varphi$
Σ^+	$\mu_B + \mu_3 + \mu_S$	$g_\Sigma^\omega \omega^0 + g_\Sigma^\phi \phi_0 + g_\Sigma^\rho \rho_0$	$M_N - g_\Sigma^s \varphi$
Σ^-	$\mu_B - \mu_3 + \mu_S$	$g_\Sigma^\omega \omega^0 + g_\Sigma^\phi \phi_0 - g_\Sigma^\rho \rho_0$	$M_N - g_\Sigma^s \varphi$
Ξ^0	$\mu_B + \frac{1}{2}\mu_3 + 2\mu_S$	$g_\Xi^\omega \omega^0 + g_\Xi^\phi \phi_0 + \frac{1}{2} g_\Xi^\rho \rho_0$	$M_N - g_\Xi^s \varphi$
Ξ^-	$\mu_B - \frac{1}{2}\mu_3 + 2\mu_S$	$g_\Xi^\omega \omega^0 + g_\Xi^\phi \phi_0 - \frac{1}{2} g_\Xi^\rho \rho_0$	$M_N - g_\Xi^s \varphi$

TABLE II. Baryon and vector meson masses (in MeV).

Baryons	Vector mesons
$M_N = 939$	$m_\omega = 782$
$M_\Lambda = 1115.6$	$m_\rho = 770$
$M_\Sigma = 1193$	$m_\phi = 1019$
$M_\Xi = 1315$	

TABLE III. $SU(3)$ relations for the relevant ω, ρ and ϕ baryon coupling constants.

Vertex	Coupling constant
$NN\omega$	$g_N^\omega = g_S \cos(\theta) + \sqrt{\frac{3}{2}} g_F \sin(\theta) - \frac{1}{\sqrt{6}} g_D \sin(\theta)$
$NN\phi$	$g_N^\phi = g_S \sin(\theta) - \sqrt{\frac{3}{2}} g_F \cos(\theta) + \frac{1}{\sqrt{6}} g_D \cos(\theta)$
$NN\rho$	$g_N^\rho = \sqrt{2}(g_F + g_D)$
$\Lambda\Lambda\omega$	$g_\Lambda^\omega = g_S \cos(\theta) - \sqrt{\frac{2}{3}} g_D \sin(\theta)$
$\Lambda\Lambda\phi$	$g_\Lambda^\phi = g_S \sin(\theta) + \sqrt{\frac{2}{3}} g_D \cos(\theta)$
$\Sigma\Sigma\omega$	$g_\Sigma^\omega = g_S \cos(\theta) + \sqrt{\frac{2}{3}} g_D \sin(\theta)$
$\Sigma\Sigma\phi$	$g_\Sigma^\phi = g_S \sin(\theta) - \sqrt{\frac{2}{3}} g_D \cos(\theta)$
$\Sigma\Sigma\rho$	$g_\Sigma^\rho = \sqrt{2} g_F$
$\Lambda\Sigma\rho$	$g_{\Lambda\Sigma}^\rho = \sqrt{\frac{2}{3}} g_D$
$\Xi\Xi\omega$	$g_\Xi^\omega = g_S \cos(\theta) - \sqrt{\frac{3}{2}} g_F \sin(\theta) - \frac{1}{\sqrt{6}} g_D \sin(\theta)$
$\Xi\Xi\phi$	$g_\Xi^\phi = g_S \sin(\theta) + \sqrt{\frac{3}{2}} g_F \cos(\theta) + \frac{1}{\sqrt{6}} g_D \cos(\theta)$
$\Xi\Xi\rho$	$g_\Xi^\rho = \sqrt{2}(g_F - g_D)$

TABLE IV. Parameter Sets. Also included is the value of the baryon density ρ_B^0 at nuclear matter equilibrium.

	G1	G2
m_s/M_N	0.53963	0.55410
$g_N^s/4\pi$	0.78532	0.83522
$g_N^\omega/4\pi$	0.96512	1.01560
$g_N^\rho/4\pi$	0.69844	0.75467
κ_3/M_N	6.3415	10.462
κ_4	-286.15	21.359
η_ω^1/M_N	0.48322	4.7310
η_ω^2	-64.952	8.3851
ζ_ω	518.48	430.26
η_ρ^1/M_n	-1.8063	2.7532
ρ_B^0 [fm^{-3}]	0.153	0.154

FIGURES

FIG. 1. Binding energy of nuclear matter. (a) at fixed isospin ratio for various strangeness ratios. The strangeness ratios are $x_S = 0.2, 0.3, 0.4, 0.5$ from the bottom to the top. (b) at fixed strangeness ratio for various isospin ratios. The isospin ratios are $x_3 = -0.1, -0.15, -0.2, -0.25$ from the bottom to the top. The parameters are based on set G1.

FIG. 2. Flavor fractions as a function of the total baryon density. The parameters are based on set G2.

FIG. 3. (a) Flavor fractions and contributions of mass eigenstates 1 and 2 to the thermodynamic potential. (b) Flavor fractions and contributions of pure Λ and Σ^0 flavors to the thermodynamic potential. The system in part (b) exhibits no flavor mixing ($x_3 = V_m = 0$).

FIG. 4. Flavor fractions of the pure strange flavors at fixed strangeness ratio for various isospin ratios. The parameters are based on set G1.

FIG. 5. Mixing density for various strangeness and isospin ratios. The parameters are based on set G2.

FIG. 6. Equation of state of neutron star matter for the two parameter sets G1 and G2.

FIG. 7. Density fractions in neutron star matter for the various baryon and lepton flavors. The parameters are based on set G2.

FIG. 8. Density ratios of the mixed Λ and Σ^0 flavors in neutron star matter.

FIG. 9. Flavor mixing frequencies and the factor $\sin(2\alpha)$ in neutron star matter.

FIGURES

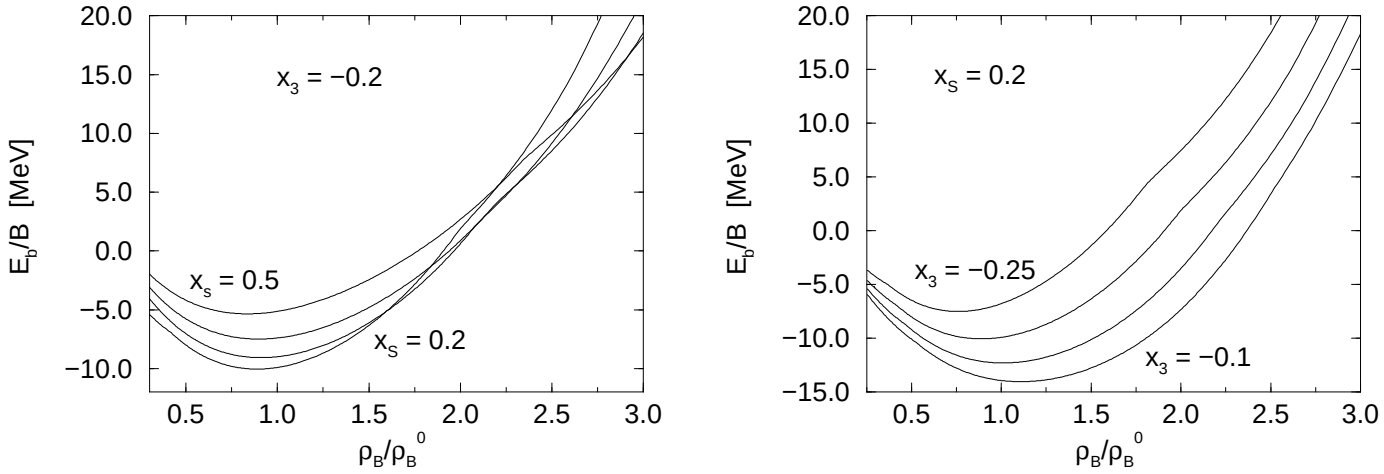

(a) (b)

FIGURE 1

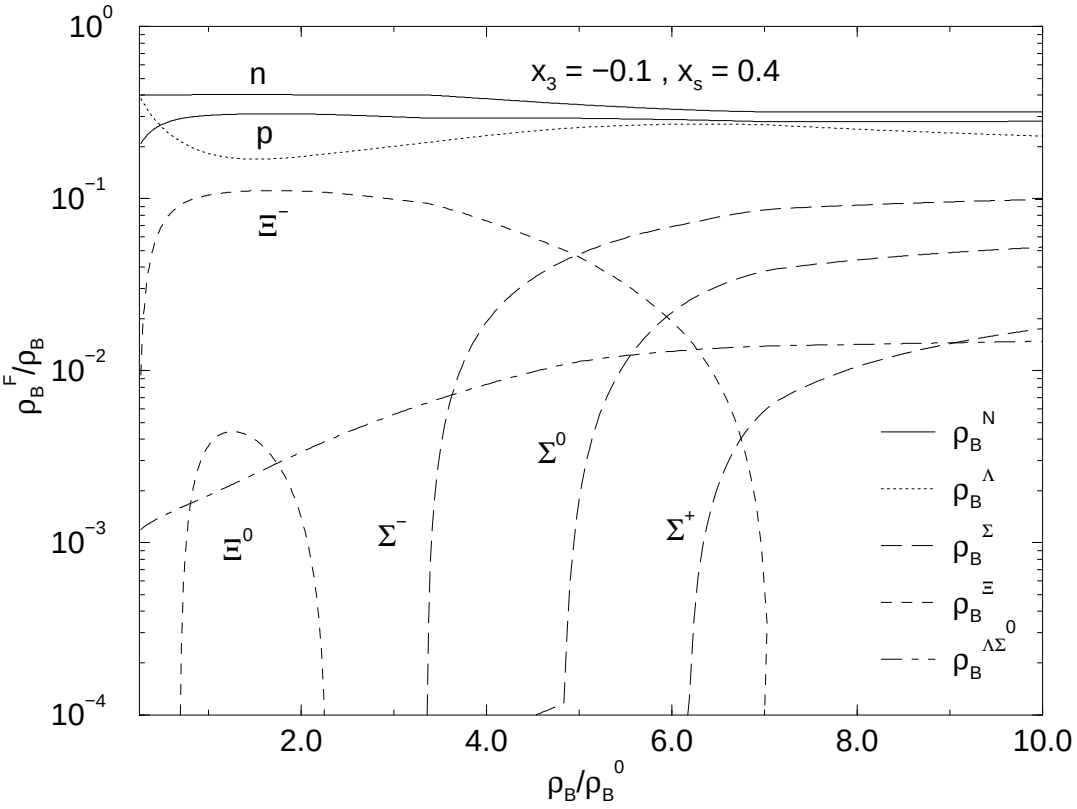
n
p
$x_3 = -0.1$, $x_s = 0.4$
Ξ^-
Ξ^0
Σ^-
Σ^0
Σ^+
ρ_B^N
ρ_B^Λ
ρ_B^Σ
ρ_B^Ξ
$\rho_B^{\Lambda\Sigma^0}$
ρ_B^F/ρ_B
ρ_B/ρ_B^0
10^0
10^{-1}
10^{-2}
10^{-3}
10^{-4}
2.0
4.0
6.0
8.0
10.0

FIGURE 2

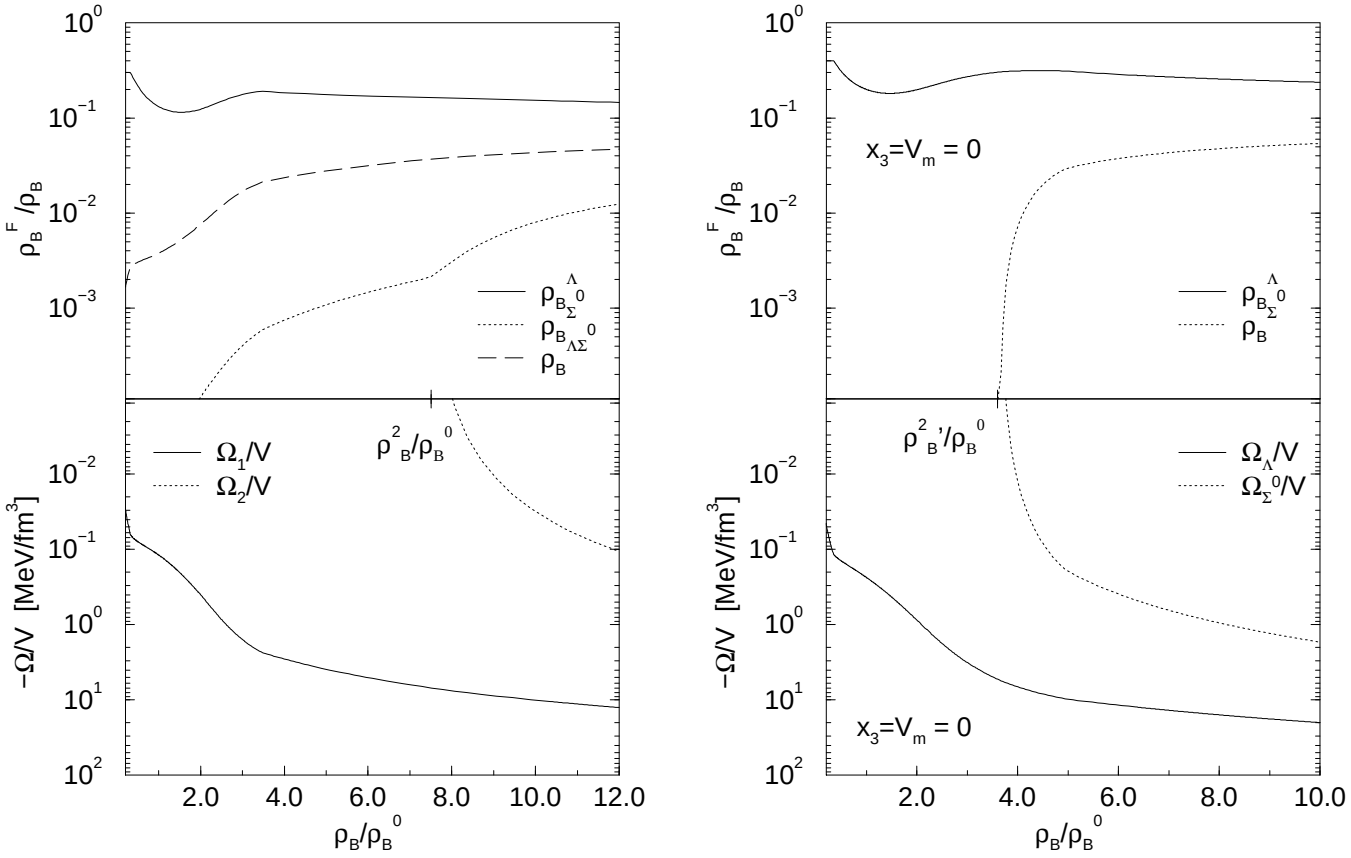
ρ_B^F/ρ_B
$\rho_{B_\Sigma}^{\Lambda\ 0}$
$\rho_{B_{\Lambda\Sigma}}{}^0$
ρ_B
Ω_1/V
Ω_2/V
$\rho^2{}_B/\rho_B{}^0$
$-\Omega/V$ [MeV/fm^3]
$\rho_B/\rho_B{}^0$
$x_3=V_m=0$
$\rho^2{}_B{}'/\rho_B{}^0$
Ω_Λ/V
$\Omega_\Sigma{}^0/V$

(a) (b)

FIGURE 3

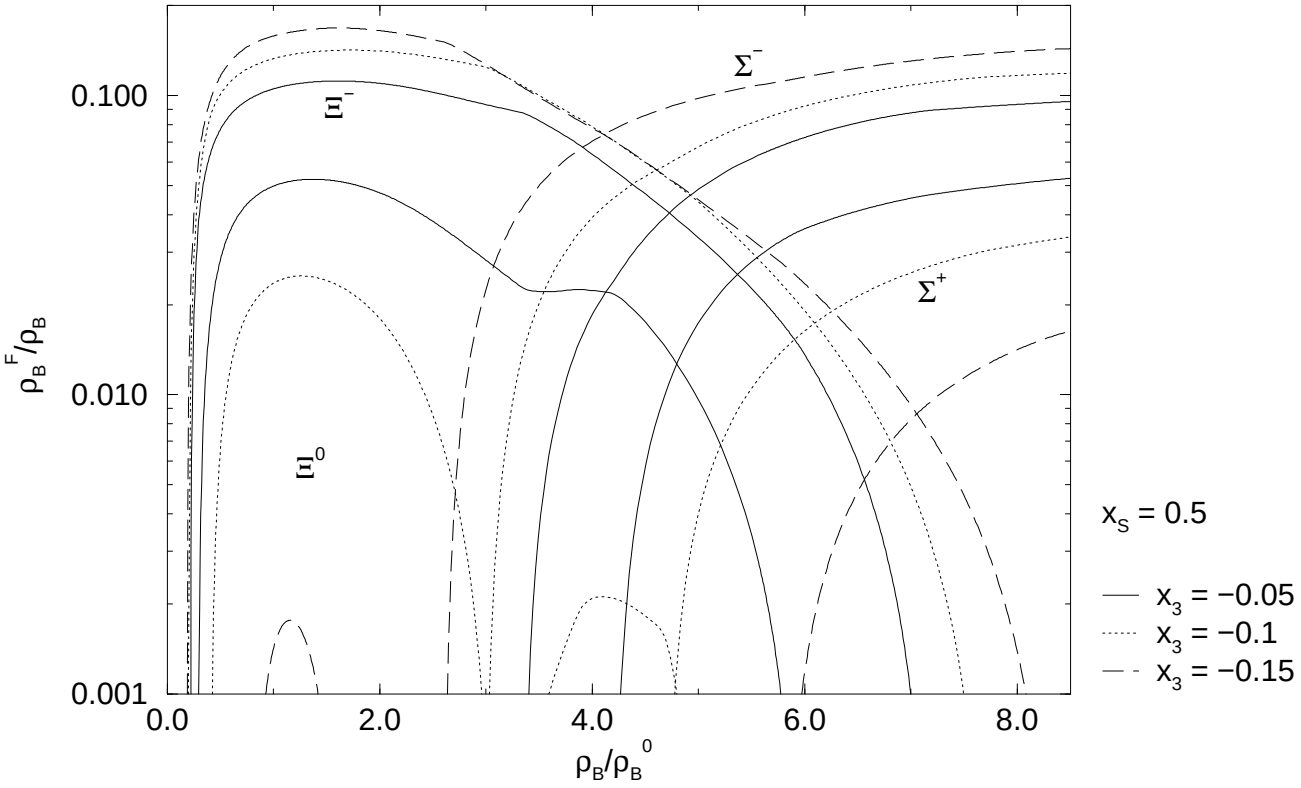
0.100
0.010
0.001
0.0
2.0
4.0
6.0
8.0
ρ_B^F/ρ_B
ρ_B/ρ_B^0
Ξ^-
Ξ^0
Σ^-
Σ^+
$x_S = 0.5$
$x_3 = -0.05$
$x_3 = -0.1$
$x_3 = -0.15$

FIGURE 4

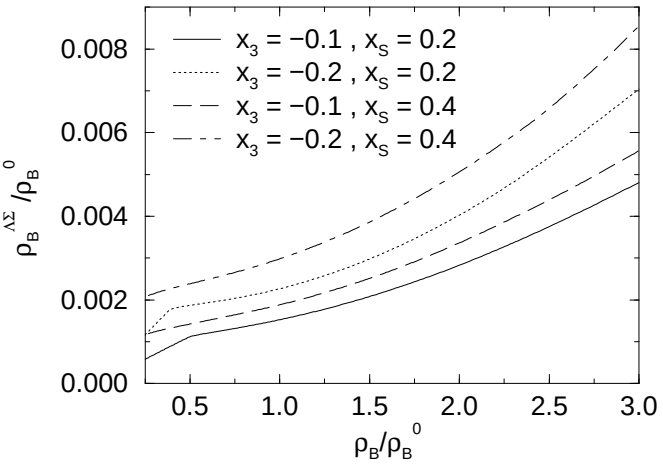
$x_3 = -0.1$, $x_S = 0.2$
$x_3 = -0.2$, $x_S = 0.2$
$x_3 = -0.1$, $x_S = 0.4$
$x_3 = -0.2$, $x_S = 0.4$
0.008
0.006
0.004
0.002
0.000
0.5
1.0
1.5
2.0
2.5
3.0
$\rho_B^{\Lambda\Sigma^0}/\rho_B^0$
ρ_B/ρ_B^0

FIGURE 5

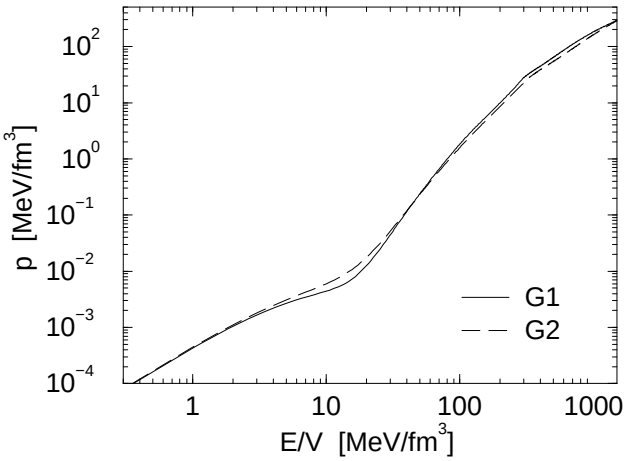

FIGURE 6

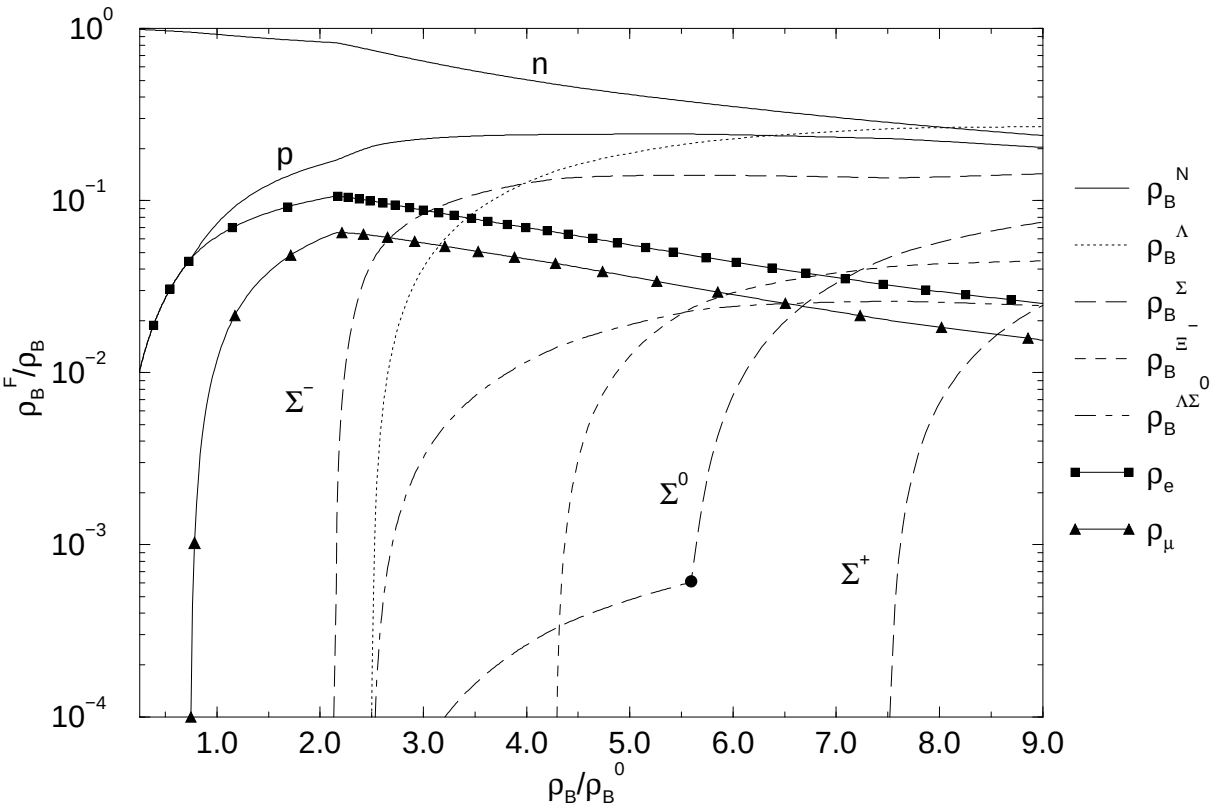
10^0
10^{-1}
10^{-2}
10^{-3}
10^{-4}
ρ_B^F/ρ_B
n
p
Σ^-
Σ^0
Σ^+
1.0
2.0
3.0
4.0
5.0
6.0
7.0
8.0
9.0
ρ_B/ρ_B^0
ρ_B^N
ρ_B^Λ
ρ_B^Σ
$\rho_B^{\Xi^-}$
$\rho_B^{\Lambda\Sigma^0}$
ρ_e
ρ_μ

FIGURE 7

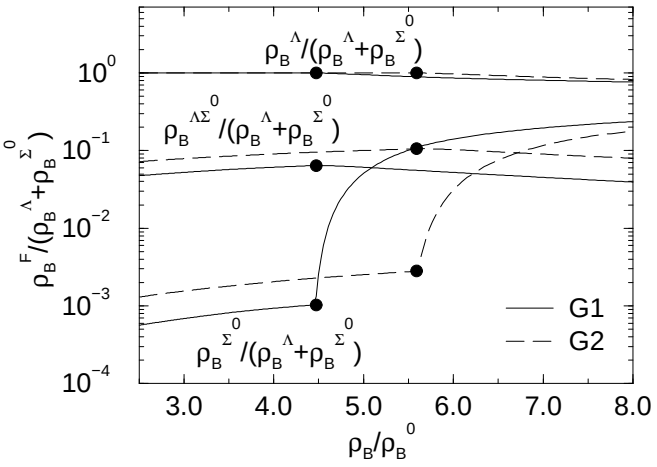
$\rho_B^{\Lambda}/(\rho_B^{\Lambda}+\rho_B^{\Sigma^0})$
$\rho_B^{\Lambda\Sigma^0}/(\rho_B^{\Lambda}+\rho_B^{\Sigma^0})$
$\rho_B^{\Sigma^0}/(\rho_B^{\Lambda}+\rho_B^{\Sigma^0})$
$\rho_B^F/(\rho_B^{\Lambda}+\rho_B^{\Sigma^0})$
ρ_B/ρ_B^0
G1
G2
10^0
10^{-1}
10^{-2}
10^{-3}
10^{-4}
3.0
4.0
5.0
6.0
7.0
8.0

FIGURE 8

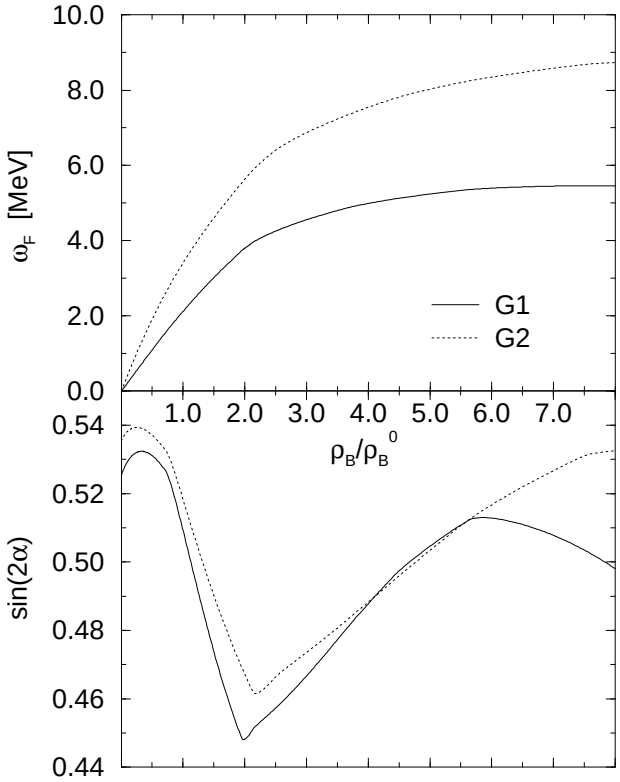
10.0
8.0
6.0
4.0
2.0
0.0
ω_F [MeV]
G1
G2
1.0 2.0 3.0 4.0 5.0 6.0 7.0
ρ_B/ρ_B^0
0.54
0.52
0.50
0.48
0.46
0.44
sin(2α)

FIGURE 9